

## Diverse Heteroleptic Ytterbium(III) Thiocyanate Complexes by Oxidation from Bis(thiocyanato)ytterbium(II)

Glen B. Deacon,\* Craig M. Forsyth, and Dallas L. Wilkinson<sup>[a]</sup>

**Abstract:** The new ytterbium(II) thiocyanate complex  $[\text{Yb}(\text{NCS})_2(\text{thf})_2]$  (**1**), synthesised by redox transmetallation between  $[\text{Hg}(\text{SCN})_2]$  and ytterbium metal in THF at room temperature, gave monomeric, eight coordinate  $[\text{Yb}(\text{NCS})_2(\text{dme})_3]$  (**2**, dme = 1,2-dimethoxyethane) on crystallisation from DME, and is a powerful, synthetically useful reductant. Thus, oxidation of **1** with  $\text{Hg}(\text{SCN})_2$ ,  $\text{Hg}(\text{C}_6\text{F}_5)_2/\text{HOdpp}$  (HOdpp = 2,6-diphenylphenol),  $\text{TICp}$  (Cp =  $\text{C}_5\text{H}_5$  or  $\text{CH}_3\text{C}_5\text{H}_4$ ),  $\text{Ti}(\text{Ph}_2\text{pz})$  ( $\text{Ph}_2\text{pz}$  = 3,5-diphenylpyrazolate) and  $\text{CCl}_3\text{CCl}_3$  in THF yielded the ytterbium(III) complexes  $[\text{Yb}(\text{NCS})_3(\text{thf})_4]$  (**3**),  $[\text{Yb}(\text{NCS})_2(\text{Odpp})(\text{thf})_3]$  (**4**),  $[\text{Yb}(\text{NCS})_2\text{Cp}(\text{thf})_3]$  (Cp =  $\text{C}_5\text{H}_5$  (**5**),  $\text{CH}_3\text{C}_5\text{H}_4$  (**6**),  $[\text{Yb}(\text{NCS})_2(\text{Ph}_2\text{pz})(\text{thf})_4]$  (**7**) and  $[\text{Yb}$

$(\text{NCS})_2\text{Cl}(\text{thf})_4]$  (**8**). In the solid state, complexes **4**, **6** and **7** were shown by X-ray crystallography to be six, eight and eight coordinate monomers, respectively. Exclusively terminal, N-bound *transoid* thiocyanate bonding is observed with  $\eta^1$ -Odpp (**4**),  $\eta^5$ - $\text{C}_5\text{H}_4\text{Me}$  (**6**) and  $\eta^2$ - $\text{Ph}_2\text{Pz}$  (**7**) ligands attached approximately perpendicular to the N...N vector. The chloride complex **8** is not a molecular species, but consists of discrete, seven coordinate  $[\text{YbCl}_2(\text{thf})_5]^+$  cations and  $[\text{Yb}(\text{NCS})_4(\text{thf})_3]^-$  anions. By contrast, oxidation of **1** with

$\text{TiO}_2\text{CPh}$  gave a mixture of  $[\{\text{Yb}(\text{NCS})(\text{O}_2\text{CPh})_2(\text{thf})_2\}_2]$  (**9**) and **3** through rearrangement of an initially formed  $[\text{Yb}(\text{NCS})_2(\text{O}_2\text{CPh})]$  species. The X-ray structure of **9** indicates a dimeric complex with a  $\{\text{Yb}(\mu\text{-O}_2\text{CPh})_4\text{Yb}\}$  core that contains both bridging bidentate and bridging tridentate benzoate groups, and with a terminal N-bound thiocyanate and two THF ligands on each ytterbium. Reduction of  $\text{Ph}_2\text{CO}$  with **1** in THF yielded the dinuclear complex  $[\{\text{Yb}(\text{NCS})_2(\text{thf})_3\}_2(\mu\text{-OC}(\text{Ph})_2\text{C}(\text{Ph})_2\text{O})]$  (**10**), in which two octahedral Yb centres are bridged by a 1,1,2,2-tetraphenylethane-1,2-diolate ligand, derived from reductive coupling of the benzophenone reagent.

**Keywords:** N ligands • O ligands • oxidation • pseudohalide • ytterbium

### Introduction

Inorganic lanthanoid(II) derivatives, and in particular the halides, have attracted considerable research interest both as key starting materials for the synthesis of a wide variety of highly reactive lanthanoid(II) species (e.g., organometallics, aryloxides and diorganoamides)<sup>[1]</sup> and also for their redox properties.<sup>[2]</sup> Thus, solutions of  $\text{SmI}_2^{[2a-c]}$  (and more recently  $\text{Sm}(\text{O}_3\text{SCF}_3)_2^{[2d, e]}$ ) in THF have extensive applications as selective one-electron reducing agents in organic syntheses, whilst  $[\text{SmI}_2(\text{thf})_2]$  is a precursor for efficient  $\text{Sm}^{\text{III}}$  Lewis acid catalysts.<sup>[2f]</sup> It should also be possible to exploit further the  $\text{Ln}^{\text{II}}/\text{Ln}^{\text{III}}$  redox couple<sup>[3]</sup> for the preparation of heteroleptic lanthanoid(III) complexes by oxidative addition to  $\text{LnX}_2$ , analogous to similar reactions of  $\text{Ln}(\text{C}_5\text{R}_5)_2$ .<sup>[1]</sup> However, this synthetic method has not been extensively explored despite

the relative scarcity of heteroleptic lanthanoid(III) complexes of the type  $[\text{LnX}_2\text{A}]$  (X = halide, A = anionic ligand)<sup>[1]</sup> and the significance of  $[\text{Sm}^{\text{III}}\text{I}_2\text{A}]$  species in the organic chemistry of  $\text{SmI}_2$ .<sup>[2]</sup> Amongst the limited examples, photolysis of solutions of  $\text{YbI}_2$  in 1,2-dimethoxyethane (DME) has been reported<sup>[4]</sup> to yield  $[\{\text{YbI}_2(\mu\text{-OMe})(\text{dme})\}_2]$ , which was shown to be an active catalyst for Meerwein–Verley–Pondorf–Oppenauer (MVPO) reactions.<sup>[4]</sup> In addition,  $\text{SmI}_2$  reductions of mercury(II)/metal carbonylates or metal carbonyls have yielded  $[\text{SmI}_2(\text{thf})_4(\mu\text{-OC})\text{Mo}(\text{CO})_2(\text{C}_5\text{H}_5)]^{[5]}$  and ionic  $[\text{SmI}_2(\text{thf})_5][\text{Co}(\text{CO})_4]^{[6]}$  respectively.

An impediment to the easy isolation of complexes of the type  $[\text{LnX}_2\text{A}]$  (X = halide) may be the poor solubility of the corresponding  $\text{LnX}_3$  derivatives in THF.<sup>[7, 8]</sup> Thus, rearrangement processes leading to mixtures of products may be thermodynamically driven by precipitation of the tris(halogeno)lanthanoid compounds, for example,  $[\text{YbI}_3(\text{thf})_4]$  was a major product from a reaction of  $[\text{YbI}_2(\text{thf})_2]$  with elemental sulphur.<sup>[8]</sup> In contrast, the pseudohalide complexes  $\text{Ln}(\text{NCS})_3$  are readily soluble in THF<sup>[9]</sup> and hence we reasoned that the “bis(thiocyanato)” ligation system could better enable iso-

[a] Prof. G. B. Deacon, Dr. C. M. Forsyth, Dr. D. L. Wilkinson  
School of Chemistry, Monash University  
Victoria 3800 (Australia)  
Fax: (+61)3-9909-4597  
E-mail: glen.deacon@sci.monash.edu.au

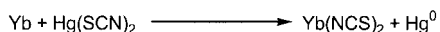
lation of  $[\text{LnX}_2\text{A}]$  ( $\text{X} = \text{NCS}$ ) species. Surprisingly, however, the reactants, lanthanoid(II) thiocyanates, for oxidative syntheses of  $[\text{Ln}(\text{NCS})_2\text{A}]$  are virtually unknown and unsolvated  $[\{\text{Eu}(\text{NCS})_2\}_n]$ , potentially the most stable homoleptic  $\text{Ln}(\text{NCS})_2$  complex, has only recently been characterised.<sup>[10]</sup>

We now report the synthesis of the new lanthanoid(II) derivative, bis(thiocyanato)ytterbium(II) and the first structural characterisation of a divalent ytterbium thiocyanate derivative,  $[\text{Yb}(\text{NCS})_2(\text{dme})_3]$ . We also report several applications of  $[\text{Yb}(\text{NCS})_2(\text{thf})_2]$  as a reducing agent to give a diverse series of complexes of the type  $[\text{Yb}(\text{NCS})_2\text{A}(\text{thf})_n]$ , and also, in one instance, a rearrangement product  $[\text{Yb}(\text{NCS})\text{A}_2(\text{thf})_n]$ . As these new functionalised lanthanoid thiocyanates are suitably crystalline, X-ray crystallographic studies provided the opportunity to examine the relative geometric influences of both the thiocyanate and the “A” ligands. Only very few  $[\text{Ln}(\text{NCS})_2\text{A}]$  or  $[\text{Ln}(\text{NCS})\text{A}_2]$  complexes have been structurally characterised, namely  $[\text{La}(\text{NCS})_2(\text{O}_2\text{CMe})\text{L}]$  ( $\text{L} = \text{N}_6$ -macrocyclic  $\text{C}_{26}\text{H}_{18}\text{N}_6$ ),<sup>[11a]</sup>  $[\text{Dy}(\text{NCS})\{\text{O}_2\text{P}(\text{OMe})\text{CH}_2\text{-(O)NEt}_2\}_2]$ <sup>[11b]</sup> and  $[\{\text{Y}(\text{HBpz}_3)(\text{NCS})(\mu\text{-OH})(\text{phen})\}_2]$ ,<sup>[11c]</sup> and there is a related polymeric “ate” complex  $[\text{Yb}(\text{C}_5\text{Me}_5)_2(\text{NCS})_2\text{K}(\text{[18]crown-6})]_n$ .<sup>[11d]</sup>

## Results and Discussion

### Syntheses and characterisation of $\text{Yb}(\text{NCS})_2$ complexes:

Reaction of mercuric thiocyanate and an excess of ytterbium metal powder in THF at room temperature gave, after 24 hours, precipitated mercury and a bright yellow solution of  $\text{Yb}(\text{NCS})_2$  (Scheme 1). After filtration of the final reaction



Scheme 1.

mixture to remove the mercury and the unreacted ytterbium, evaporation of the yellow solution to dryness gave a brick-red, air-sensitive solid which was identified (see below) as  $[\text{Yb}(\text{NCS})_2(\text{thf})_2]$  (**1**). Prior to complete removal of the solvent, large yellow crystals were obtained, but when these were removed from the supernatant THF solution their colour rapidly changed to red. This behaviour is indicative of facile loss of coordinated solvent (thf) and suggests that the yellow complex is an unstable higher solvate  $[\text{Yb}(\text{NCS})_2(\text{thf})_n]$ ,  $n > 2$ . Recrystallisation of **1** from DME also gave yellow crystals which were identified as  $[\text{Yb}(\text{NCS})_2(\text{dme})_3]$  (**2**). This compound remained yellow, even when heated (ca. 50 °C) under vacuum, and its stability, relative to the yellow THF complex, can be presumably related to the bidentate coordination of DME (see below).

The compositions of **1** and **2** were established by elemental analyses (Yb or C, H) and the presence of divalent ytterbium in **1** was inferred from the absence of characteristic ytterbium(III)  $f \leftarrow f$  transitions near 1000 nm<sup>[12]</sup> in the near infrared spectrum. The most prominent features of the infrared spectra of **1** and **2** are strong absorptions near 2100 cm<sup>-1</sup> attributable to carbon–nitrogen stretching of a thiocyanate group. The position of the major  $\nu(\text{CN})$  band of **2** (2057 cm<sup>-1</sup>) as well as

the  $\nu(\text{CS})$  absorptions (863 and 855 cm<sup>-1</sup>) are in the region expected for a N-bonded metal–thiocyanate complex;<sup>[13]</sup> this was confirmed by the single-crystal structure determination (see below). However, the significantly higher value of  $\nu(\text{CN})$  for **1** (2087 cm<sup>-1</sup>) may indicate a different bonding mode in this complex<sup>[13]</sup> (see below). The infrared spectra also exhibited strong to medium intensity absorptions associated with the coordinated solvents (e.g., THF in **1** at 1027, 876 cm<sup>-1</sup> and DME in **2** at 1062 cm<sup>-1</sup>).<sup>[14]</sup> The <sup>171</sup>Yb{<sup>1</sup>H} NMR of **1** in THF gave a single, broad resonance at  $\delta = 340$ . In this form, the ytterbium is likely to be maximally solvated by THF and probably exists as  $[\text{Yb}(\text{NCS})_2(\text{thf})_n]$  ( $n = 4$ ). The chemical shift value is more closely allied with that of inorganic  $[\text{YbI}_2(\text{thf})_4]$  ( $\delta$  (<sup>171</sup>Yb) = 456)<sup>[15]</sup> rather than those of ytterbium(II) complexes with amide ligands (e.g.,  $[\text{Yb}\{\text{N}(\text{SiMe}_3)_2\}_2\text{L}]$  species have  $\delta$  (<sup>171</sup>Yb) > 600<sup>[16]</sup>), consistent with the pseudohalide nature of  $\text{SCN}^-$ .

**The X-ray structure of  $[\text{Yb}(\text{NCS})_2(\text{dme})_3]$  (**2**):** The molecular structure of **2** is shown in Figure 1 and selected bond lengths and angles are listed in Table 1. Monomeric **2** is sited on a

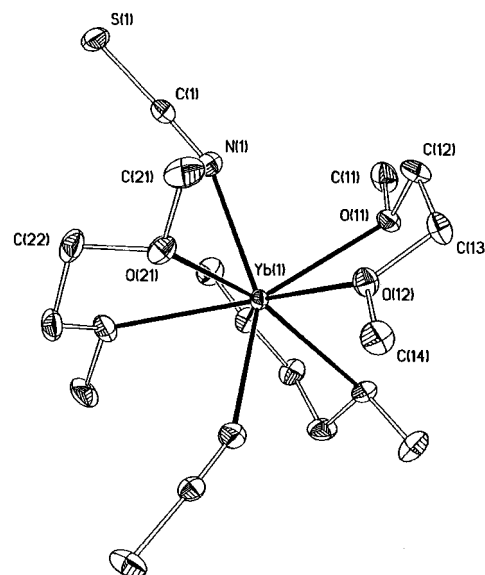


Figure 1. The X-ray structure of  $[\text{Yb}(\text{NCS})_2(\text{dme})_3]$  (**2**); 50% thermal ellipsoids are shown for the non-hydrogen atoms; hydrogen atoms have been omitted for clarity.

Table 1. Selected bond lengths [Å] and angles [°] for  $[\text{Yb}(\text{NCS})_2(\text{dme})_3]$  (**2**).

Yb(1)–N(1)	2.481(2)	Yb(1)–O(12)	2.465(2)
Yb(1)–O(11)	2.590(2)	Yb(1)–O(21)	2.578(2)
O(11)–Yb(1)–O(21A) <sup>[a]</sup>	151.19(6)	O(21)–Yb(1)–N(1A) <sup>[a]</sup>	80.38(8)
N(1)–Yb(1)–N(1A) <sup>[a]</sup>	148.6(1)	O(12)–Yb(1)–O(21)	76.22(7)
O(12)–Yb(1)–O(12A) <sup>[a]</sup>	144.09(9)	N(1)–Yb(1)–O(11)	75.24(7)
O(12)–Yb(1)–O(21A) <sup>[a]</sup>	138.89(6)	N(1)–Yb(1)–O(21)	73.41(7)
O(11)–Yb(1)–N(1A) <sup>[a]</sup>	134.15(7)	O(11)–Yb(1)–O(12)	64.27(6)
O(11)–Yb(1)–O(21)	119.15(7)	O(21)–Yb(1)–O(21A) <sup>[a]</sup>	66.6(1)
N(1)–Yb(1)–O(12)	105.85(8)	Yb(1)–N(1)–C(1)	155.9(2)
O(11)–Yb(1)–O(12A) <sup>[a]</sup>	86.05(7)	N(1)–C(1)–S(1)	177.9(3)
O(12)–Yb(1)–N(1A) <sup>[a]</sup>	83.91(8)		

[a] Symmetry transformations used to generate equivalent atoms:  $-x, y, -z + 3/2$ .

crystallographic twofold axis through Yb(1) and the midpoint of the C(22)–C(22A) bond. The ytterbium environment is eight coordinate with two N-bonded thiocyanate anions and three chelating DME ligands; the geometry of the donor atoms is distorted dodecahedral. The Yb–N bond lengths in **2** (Table 1) compare well with those of the monomeric ytterbium(III) thiocyanate complex  $[\text{Yb}(\text{NCS})_3(\text{thf})_4]$  ( $\langle \text{Yb–N} \rangle$  2.274 Å)<sup>[9]</sup> after accounting for the 0.215 Å difference in the respective metal ionic radii.<sup>[17]</sup> Similarly, the M–O(dme) bond lengths in **2** (Table 1) and eight coordinate  $[\text{SmI}_2(\text{dme})_3]$  ( $\langle \text{Sm–O}(\text{dme}) \rangle$  2.676 Å)<sup>[18]</sup> are comparable given that  $\text{Sm}^{2+}$  is 0.13 Å larger than  $\text{Yb}^{2+}$ .<sup>[17]</sup> The overall structural appearance of **2** is similar to that of the “bent” form of  $[\text{SmI}_2(\text{dme})_3]$ .<sup>[18]</sup> However, for the smaller thulium and ytterbium there is a change in the coordination number to seven in  $[\text{TmI}_2(\text{dme})_3]$ ,<sup>[19a]</sup> in which one of the DME ligands is coordinated by one oxygen only, and seven in  $[\{\text{YbI}_2(\text{dme})_2\}_2(\mu\text{-dme})]$ ,<sup>[19b]</sup> which has a bridging bidentate (O:O') DME, but in a bridging mode. Thus, in the current structure, it appears that a coordination number of eight is attained owing to the smaller size of thiocyanate than iodide.<sup>[20]</sup>

For **1**, a monomeric and four coordinate structure would appear to be very sterically unsaturated (sum of ligand steric coordination numbers = 4.2<sup>[20]</sup>), and for the large lanthanoid(III) cations, this structural type  $[\text{YbA}_2(\text{thf})_2]$  is typically observed only with very bulky anions (e.g.,  $\text{A} = \text{OC}_6\text{H}_2\text{-2,6-}i\text{Bu}_2\text{-4-Me}$ ,<sup>[21]</sup> (sum of ligand steric coordination numbers = 7.2<sup>[20]</sup>), or  $\text{N}(2,6\text{-}i\text{Pr}_2\text{C}_6\text{H}_3)(\text{SiMe}_3)$ <sup>[22]</sup>). Further,  $[\{\text{SmI}_2\text{L}_2\}_n]$  ( $\text{L} = \text{NCrBu}$ )<sup>[23]</sup> is polymeric with bridging iodides and approximately octahedral stereochemistry. Thus, **1** is likely to have an associated structure (e.g., Figure 2a) probably with

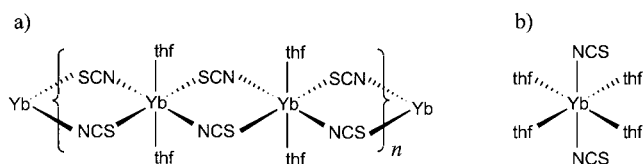


Figure 2. Proposed structures of  $[\{\text{Yb}(\text{NCS})_2(\text{thf})_2\}_n]$  and  $[\text{Yb}(\text{NCS})_2(\text{thf})_4]$ .

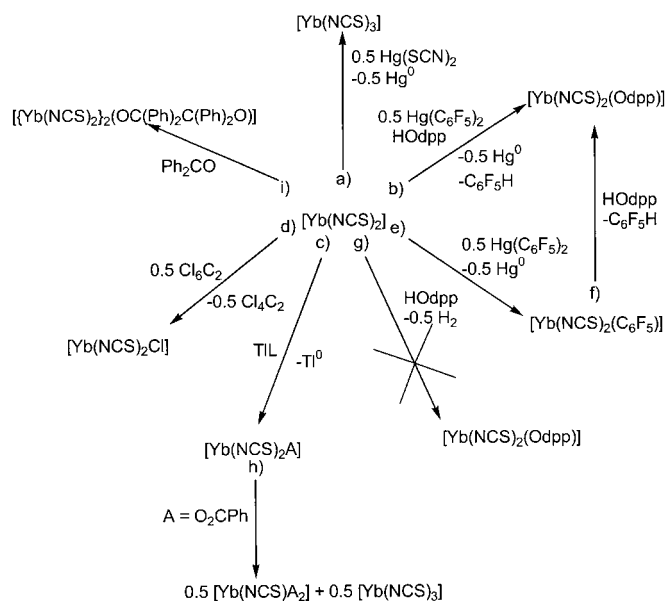
Yb–NCS–Yb bridges similar to the bonding observed in  $[\{\text{Ln}(\text{NCS})_3(\text{thf})_4\}_2]$  ( $\text{Ln} = \text{Nd}, \text{Eu}, \text{Er}$ ).<sup>[24]</sup> The value of  $\nu(\text{CN})$  for **1** is in the region typical of this bonding mode.<sup>[13]</sup> By analogy with the observed octahedral structure of  $\text{trans-}[\text{Ca}(\text{NCS})_2(\text{thf})_4]$ <sup>[25]</sup> ( $\text{Ca}^{2+}$  and  $\text{Yb}^{2+}$  have nearly identical ionic radii<sup>[17]</sup>), the unstable yellow crystals of “ $[\text{Yb}(\text{NCS})_2(\text{thf})_n]$ ” are likely to be of a monomeric and six coordinate complex, that is,  $\text{trans-}[\text{Yb}(\text{NCS})_2(\text{thf})_4]$  (Figure 2b). Further, the steric demands of four THF ligands are similar to those of three chelating DME ligands (in **2**).<sup>[20]</sup>

**Oxidation reactions of  $\text{Yb}(\text{NCS})_2$ :** We initially investigated the reaction of **1** with mercury(II) thiocyanate in THF, which gave the known trivalent ytterbium complex  $[\text{Yb}(\text{NCS})_3(\text{thf})_4]$ <sup>[9]</sup> (**3**) (Table 2; Scheme 2 route a). This established that oxidation of **1** was facile and, therefore, potentially amenable to the synthesis of functionalised bis(thiocyanato)ytterbium(III) derivatives. Thus, we have explored several oxidations

Table 2. Oxidation reactions of  $[\text{Yb}(\text{NCS})_2(\text{thf})_2]$  (**1**).

<b>1</b> [mmol]	Reagent [mmol]	THF [mL]	Time [h]	Product (% yield)
2.0	Hg(SCN) <sub>2</sub> (1.0)	20	16	<b>3</b> (52)
2.0	Hg(C <sub>6</sub> F <sub>5</sub> ) <sub>2</sub> (1.0) HOdpp (2.0)	40	5d	<b>4</b> (41)
2.0	Tl(C <sub>3</sub> H <sub>5</sub> ) (2.0)	40	16	<b>5</b> (36)
2.0	Tl(C <sub>3</sub> H <sub>4</sub> Me) (2.0)	25	16	<b>6</b> (43)
2.0	Tl(Ph <sub>2</sub> pz) (2.0)	20	16	<b>7</b> (46)
2.0	Cl <sub>3</sub> CCl <sub>3</sub> (2.0)	30	1	<b>8</b> (72)
1.0	Tl(O <sub>2</sub> CPh) (1.0)	40	16	<b>9</b> (74) <sup>[a]</sup> <b>3</b> <sup>[b]</sup>
2.0	Ph <sub>2</sub> CO (2.0)	30	16	<b>10</b> (43)

[a] Based on reactions c and h in Scheme 2. [b] Yield not determined.



Scheme 2.

of **1** and have obtained a diverse series of complexes of the general type  $[\text{Yb}(\text{NCS})_2\text{A}(\text{thf})_n]$  ( $\text{A} = \text{Odpp}$  (2,6-diphenylphenolate),  $n = 3$ , **4**;  $\text{A} = \text{C}_5\text{H}_5$ ,  $n = 3$ , **5**;  $\text{A} = \text{CH}_3\text{C}_5\text{H}_4$ ,  $n = 3$ , **6**;  $\text{A} = \text{Ph}_2\text{pz}$  (3,5-diphenylpyrazolate),  $n = 4$ , **7**;  $\text{A} = \text{Cl}$ ,  $n = 4$ , **8**). These were achieved using a variety of reagents (Table 2) including  $\text{Hg}(\text{C}_6\text{F}_5)_2$ , in the presence of a protic reagent (Scheme 2 route b,  $\text{A} = \text{Odpp}$ ), thallium(I) compounds (Scheme 2 route c,  $\text{A} = \text{C}_5\text{H}_5$ ,  $\text{CH}_3\text{C}_5\text{H}_4$ ,  $\text{Ph}_2\text{pz}$ ) and an organic oxidant, hexachloroethane (Scheme 2 route d). The formation of the Odpp derivative (Scheme 2 route b) is presumed to occur by initial oxidation of **1** by  $\text{Hg}(\text{C}_6\text{F}_5)_2$  (e.g., Scheme 2 route e) followed by rapid protolysis of the intermediate “ $\text{Yb}(\text{NCS})_2(\text{C}_6\text{F}_5)$ ” species by the phenol (Scheme 2 route f). We have shown that HOdpp does not oxidise **1** directly (Scheme 2 route g).

In an attempt to prepare a bis(thiocyanato)ytterbium(III) carboxylate complex, **1** was treated with  $\text{Tl}(\text{O}_2\text{CPh})$  in THF. Rapid deposition of Tl metal was observed, consistent with route c, but the product subsequently crystallised proved instead to be a bis(carboxylato)ytterbium(III) thiocyanate,  $[\{\text{Yb}(\text{NCS})(\text{O}_2\text{CPh})_2(\text{thf})_2\}_2]$  (**9**), as established by X-ray crystallography. This outcome may be explained by rearrange-

ment of an initially formed [Yb(NCS)<sub>2</sub>(O<sub>2</sub>CPh)] species (Scheme 2 route c) giving [Yb(NCS)(O<sub>2</sub>CPh)<sub>2</sub>] and Yb(NCS)<sub>3</sub> (Scheme 2 route h). The formation of the latter was subsequently established by crystallisation of [Yb(NCS)<sub>3</sub>(thf)<sub>4</sub>] (**3**) from the filtrate of separate preparation after removal of **9**. The cell constants obtained for **3** (see Experimental Section) were similar to room temperature data reported for this complex.<sup>[9]</sup> The small contraction of the cell is presumably due to the lower temperature (123 K) of the current measurement.

The reaction of **1** with benzophenone was investigated since ketones are common substrates in SmI<sub>2</sub>-mediated transformations of organic compounds.<sup>[2]</sup> In the present case, instantaneous formation of a pale purple precipitate was observed. This dissolved upon subsequent heating, and cooling of the resulting intense red solution deposited colourless crystals of [{Yb(NCS)<sub>2</sub>(thf)<sub>3</sub>]<sub>2</sub>(μ-OC(Ph)<sub>2</sub>C(Ph)<sub>2</sub>O)·THF (**10**) (Scheme 2 route i). This complex contains a 1,1,2,2-tetraphenylethane-1,2-diolate ligand derived from reductive coupling of Ph<sub>2</sub>CO. Analogous products (e.g., [{SmA<sub>2</sub>L<sub>x</sub>]<sub>2</sub>(μ-pinacolate)], pinacolate = 1,2-bis(biphenyl-2,2'-diyl)ethane-1,2-diolate; A = OC<sub>6</sub>H<sub>2</sub>-2,6-*t*Bu<sub>2</sub>-4-Me, L<sub>x</sub> = OEt<sub>2</sub>; A = N(SiMe<sub>3</sub>)<sub>2</sub>, L<sub>x</sub> = (thf)<sub>2</sub> or (hmpa)<sub>2</sub> HMPA = hexamethylphosphoric triamide) have been isolated from reactions of SmA<sub>2</sub> and fluorenone.<sup>[26]</sup> These were shown to result from radical coupling of lanthanoid(III) ketyl complexes, generated by single-electron transfer from the divalent lanthanoids to the C=O functionality.<sup>[26, 27]</sup> Furthermore, the central C–C bond of these pinacolate species could be cleaved by addition of a strongly coordinating solvent (e.g., THF or THF/HMPA), regenerating the highly coloured ketyl complexes. Whilst dissolution of the initial precipitate formed during the preparation of **10** gave a highly coloured red solution, suggestive of the presence of a ketyl species, heating of the *isolated* complex in THF gave a near colourless solution with a UV-visible spectrum inconsistent with the presence of a ketyl species.<sup>[26]</sup> It is interesting to note that reactions of benzophenone with bulky aryloxolanthanoid(II) reducing agents did not yield pinacolate complexes, but rather hydrogen-atom abstraction products (e.g., [Yb(OCHPh)<sub>2</sub>]<sub>2</sub>A(HMPA)], A = OC<sub>6</sub>H<sub>2</sub>-2,6-*t*Bu<sub>2</sub>-4-Me).<sup>[26]</sup> Presumably, the considerably larger size of the aryloxide ligands (relative to thiocyanate) inhibits coupling of the initially formed lanthanoid ketyl complex. Thus, the current isolation of **10** more closely represents the chemistry of SmI<sub>2</sub> mediated organic reactions and indeed **10** is the first crystallographically characterised (see below) lanthanoid pinacolate with halide/pseudohalide co-ligands.

The compositions of the oxidation products (Table 2) were established by elemental analyses (see Experimental Section). The C, H, N microanalyses for **7** were closer to those calculated for the composition [Yb(NCS)<sub>2</sub>(Ph<sub>2</sub>pz)(thf)<sub>3</sub>] rather than [Yb(NCS)<sub>2</sub>(Ph<sub>2</sub>pz)(thf)<sub>4</sub>], as indicated by metal analysis and established by X-ray crystallography. Possibly, dissociation of THF occurred during preparation and transport of the microanalysis sample. An analytically pure sample of **9** could not be obtained due to persistent contamination with the [Yb(NCS)<sub>3</sub>(thf)<sub>4</sub>] byproduct. The presence of trivalent ytterbium in representative complexes was indicated by two weak near-infrared absorptions at 925(±2) and

975(±2) nm in their electronic spectra, attributable to Yb<sup>III</sup> f ← f transitions.<sup>[12]</sup> The cyclopentadienyl complex **5** also displayed a charge-transfer absorption in the visible region at 448 nm accounting for the intense orange colour, in contrast to the colourless or pale yellow appearance of most other products. Meaningful NMR data for these complexes were not accessible owing to severe broadening and shifting by the paramagnetism of the Yb<sup>III</sup> oxidation state.<sup>[28]</sup> The infrared spectra of **3–8** and **10** exhibited a very narrow range (2050–2039 cm<sup>-1</sup>) for the ν(CN) absorptions suggesting similar thiocyanate bonding for each of these complexes, and the position is typical for terminal N-bound metal thiocyanates.<sup>[13]</sup> The spectrum of **3** agreed with literature data for this compound.<sup>[9]</sup> For **9**, the position of the ν(CN) frequency was higher, suggestive of a possible structural variation in this complex (see below). Bands attributable to coordinated THF<sup>[14]</sup> were observed at 1010–1030 cm<sup>-1</sup> and 840–880 cm<sup>-1</sup> in each spectrum. Furthermore, characteristic bands attributable to lanthanoid-bound Odpp,<sup>[29]</sup> C<sub>5</sub>H<sub>4</sub>R (R = H, Me)<sup>[14]</sup> and Ph<sub>2</sub>Pz<sup>[30, 31]</sup> ligands were evident in the spectra of the respective compounds. For the benzoate **9**, strong absorptions at 1618 and 1571 cm<sup>-1</sup> were identified as possible ν<sub>as</sub>(CO<sub>2</sub>) bands, the lower energy absorption overlapping a weaker aryl ν(C=C). These could be associated with the two different bridging benzoate groups present in **9** (see below). Comparative data reported for [Ln(HBpz<sub>3</sub>)<sub>2</sub>(O<sub>2</sub>CPh)] (KBr pellet) showed three spectral variations depending on the lanthanoid.<sup>[32]</sup> The current data were similar to those of Ln = La, Nd, Sm, Eu (1605, 1560 cm<sup>-1</sup>), whilst the Yb and Lu analogues had a different infrared absorption with only one strong band (1525 cm<sup>-1</sup>) in the ν<sub>as</sub>(CO<sub>2</sub>) region. The ytterbium complex [Yb(HBpz<sub>3</sub>)<sub>2</sub>(O<sub>2</sub>CPh)] was shown to be monomeric with a chelating benzoate coordination mode.<sup>[32]</sup> In a separate study, the Sm derivative was shown to be dimeric with bridging bidentate benzoate ligands,<sup>[33]</sup> but the reported infrared spectrum for this complex had only one ν<sub>as</sub>(CO<sub>2</sub>) absorption (1520 cm<sup>-1</sup>) in contrast to the earlier data<sup>[32]</sup> and also that of the analogous dimer [{Sm(C<sub>5</sub>Me<sub>5</sub>)<sub>2</sub>(μ-O<sub>2</sub>CPh)]<sub>2</sub> (1597, 1553 cm<sup>-1</sup>).<sup>[34]</sup>

**X-ray structure determinations:** The oxidation products were characterised by single-crystal X-ray structure determinations. Crystals were grown from solutions that contained a vast excess of THF (either neat THF or THF/light petroleum mixtures) and accordingly are presumably maximally solvated. Selected geometrical parameters for each complex are listed in Tables 3–8 and cell constants and refinement details are listed in the Experimental Section (Table 9). Crystals of the cyclopentadienyl complex **5** were obtained but were invariably twinned. However, the structure is likely to be analogous to that of the methyl-substituted derivative **6**. In general, the thiocyanate ligands were found to be terminal and bound to ytterbium through the nitrogen atom.

**Monomeric [Yb(NCS)<sub>2</sub>A(thf)<sub>n</sub>] complexes **4**, **6** and **7**:** In [Yb(NCS)<sub>2</sub>(Odpp)(thf)<sub>3</sub>] (**4**) (Figure 3), the central ytterbium atom is six coordinate, surrounded by an oxygen-bound diphenylphenolate, two *transoid* thiocyanates and three *mer* THF ligands, with distorted octahedral geometry. By contrast,

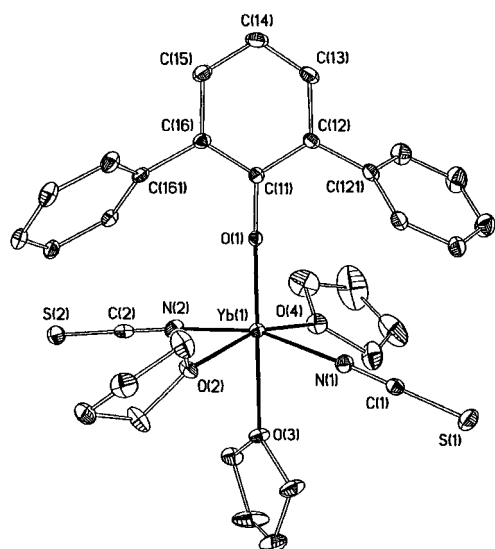


Figure 3. The X-ray structure of  $[\text{Yb}(\text{NCS})_2(\text{Odpp})(\text{thf})_3]$  (**4**); 30% thermal ellipsoids are shown for the non-hydrogen atoms; hydrogen atoms have been omitted for clarity.

$[\text{Yb}(\text{NCS})_2(\text{MeC}_5\text{H}_4)(\text{thf})_3]$  (**6**) (Figure 4) is formally eight coordinate, with an  $\eta^5$ -methylcyclopentadienyl, two *transoid* thiocyanates and three *mer* THF ligands coordinated to ytterbium. If the centroid ( $C_c$ ) of the  $C_5$  ring is considered to occupy a single geometric vertex, the ytterbium coordination

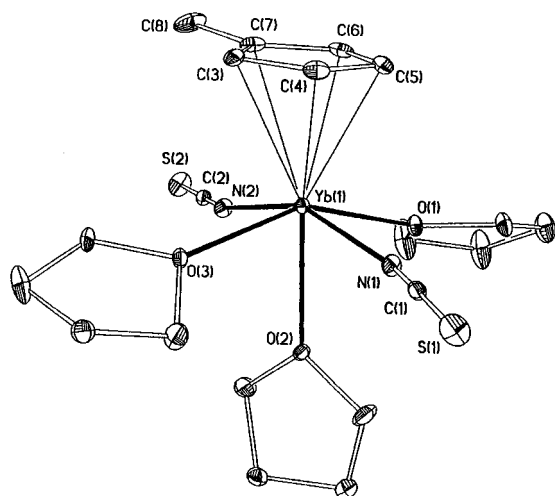


Figure 4. The X-ray structure of  $[\text{Yb}(\text{NCS})_2(\text{CH}_5\text{C}_5\text{H}_4)(\text{thf})_3]$  (**6**); 30% thermal ellipsoids are shown for the non-hydrogen atoms; hydrogen atoms have been omitted for clarity.

environment can be described as pseudo-octahedral, and is therefore similar to that of the Odpp complex. Further,  $[\text{Yb}(\text{NCS})_2(\text{Ph}_2\text{pz})(\text{thf})_4]$  (**7**) (Figure 5) is also eight coordinate with an  $\eta^2$ - $\text{Ph}_2\text{pz}$ , two *transoid* thiocyanates and four coordinated THF ligands. The ytterbium atom and the central carbon, C(3), of the pyrazolate ring reside on a crystallographic twofold axis. The  $\eta^2$ -pyrazolate coordination mode is typical for lanthanoid– $\text{Ph}_2\text{pz}$  complexes,<sup>[30, 31]</sup> and it is common to model the coordination as a single site at the midpoint of the N–N bond (designated as  $N_c$ ), since the very small bite angle ( $34.3(1)^\circ$ ) of the pyrazolate severely distorts any regular

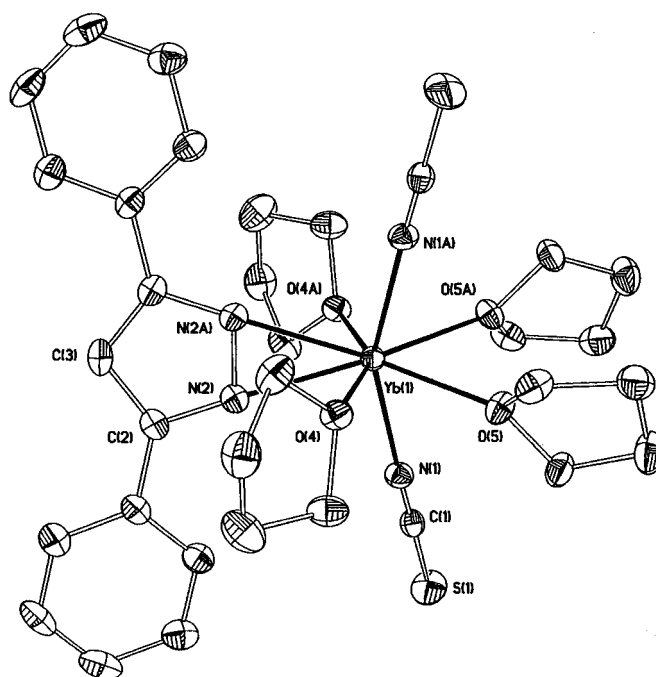


Figure 5. The X-ray structure of  $[\text{Yb}(\text{NCS})_2(\text{Ph}_2\text{pz})(\text{thf})_4]$  (**7**); 30% thermal ellipsoids are shown for the non-hydrogen atoms; hydrogen atoms have been omitted for clarity.

polyhedron. Thus, the ytterbium coordination geometry in **7** can be described as a pseudo-pentagonal bipyramid with axial thiocyanate ligands and equatorial THF,  $N_c$  and NCS groups, an arrangement which is similar to that of  $[\text{Yb}(\text{NCS})_3(\text{thf})_4]$ ,<sup>[9]</sup> despite the significant difference in the relative sizes of the  $\text{Ph}_2\text{pz}$  and NCS ligands.

A common feature of these three structures is the exclusively *transoid* arrangement of thiocyanate ligands. However, the nitrogen atoms of the thiocyanate ligands are not exactly linearly disposed about the ytterbium centres, but are significantly bent with N–Yb–N angles ranging from  $155.7(2)$  to  $163.4(2)^\circ$  (Tables 3–5). Furthermore, for the

Table 3. Selected bond lengths [Å] and angles [ $^\circ$ ] for  $[\text{Yb}(\text{NCS})_2(\text{Odpp})(\text{thf})_3]$  (**4**).

Yb(1)–N(1)	2.282(5)	Yb(1)–O(2)	2.277(4)
Yb(1)–N(2)	2.295(5)	Yb(1)–O(3)	2.357(4)
Yb(1)–O(1)	2.025(3)	Yb(1)–O(4)	2.282(4)
N(1)–Yb(1)–N(2)	163.4(2)	O(2)–Yb(1)–O(4)	162.8(2)
O(1)–Yb(1)–O(3)	179.4(1)		
O(1)–Yb(1)–N(1)	99.0(2)	O(3)–Yb(1)–N(1)	81.3(2)
O(1)–Yb(1)–N(2)	97.5(2)	O(3)–Yb(1)–N(2)	82.1(2)
O(1)–Yb(1)–O(2)	98.9(1)	O(3)–Yb(1)–O(2)	81.6(1)
O(1)–Yb(1)–O(4)	98.1(2)	O(3)–Yb(1)–O(4)	81.4(2)

octahedral or pseudo-octahedral complexes **4** and **6** the *transoid*-O(thf)–Yb–O(thf) angles are similarly nonlinear and there is an opening of the *cis*-O(OAr)–Yb–X and *cis*- $C_c$ –Yb–X (X = N, O(thf)) angles (Tables 3 and 4). Thus, the equatorial girdle of thiocyanate and THF ligands has been displaced toward the axial THF presumably by the steric bulk

Table 4. Selected bond lengths [Å] and angles [°] for [Yb(NCS)<sub>2</sub>-(C<sub>3</sub>H<sub>4</sub>Me)(thf)<sub>3</sub>] (**6**).

Yb(1)–C(3)	2.662(4)	Yb(1)–N(1)	2.292(4)
Yb(1)–C(4)	2.616(5)	Yb(1)–N(2)	2.282(4)
Yb(1)–C(5)	2.586(5)	Yb(1)–O(1)	2.334(3)
Yb(1)–C(6)	2.615(4)	Yb(1)–O(2)	2.426(3)
Yb(1)–C(7)	2.687(5)	Yb(1)–O(3)	2.328(3)
N(1)–Yb(1)–N(2)	155.7(1)	O(1)–Yb(1)–O(3)	151.3(1)
Ct–Yb(1)–O(2)	179.3(3)		
Ct–Yb(1)–N(1)	102.2(3)	N(1)–Yb(1)–O(2)	77.7(1)
Ct–Yb(1)–N(2)	102.0(3)	N(2)–Yb(1)–O(2)	77.9(1)
Ct–Yb(1)–O(1)	104.4(3)	O(1)–Yb(1)–O(2)	74.9(1)
Ct–Yb(1)–O(3)	104.3(3)	O(2)–Yb(1)–O(3)	76.4(1)

Table 5. Selected bond lengths [Å] and angles [°] for [Yb(NCS)<sub>2</sub>(Ph<sub>2</sub>pz)(thf)<sub>4</sub>] (**7**).

Yb(1)–N(1)	2.302(3)	Yb(1)–O(4)	2.387(2)
Yb(1)–N(2)	2.319(3)	Yb(1)–O(5)	2.407(2)
O(4)–Yb(1)–N <sub>i</sub>	76.1(1)	O(4)–Yb(1)–O(4A) <sup>[a]</sup>	152.1(1)
O(4)–Yb(1)–O(5)	68.85(9)	O(4)–Yb(1)–O(5A) <sup>[a]</sup>	138.76(9)
O(5)–Yb(1)–O(5A) <sup>[a]</sup>	71.5(1)	O(5)–Yb(1)–N <sub>i</sub>	144.3(1)
N(1)–Yb(1)–O(4)	101.2(1)	N(1)–Yb(1)–N(1A) <sup>[a]</sup>	157.1(2)
N(1)–Yb(1)–O(5)	79.49(9)	N(1)–Yb(1)–N <sub>i</sub>	101.5(1)

[a] Symmetry transformations used to generate equivalent atoms:  $-x, y, -z + 1/2$ .

of the A ligand (Steric CN: Odpp (1.9),<sup>[35a]</sup> MeC<sub>5</sub>H<sub>4</sub> (2.14),<sup>[20]</sup> Ph<sub>2</sub>pz (1.7),<sup>[35b]</sup> THF (1.21),<sup>[20]</sup> NCS (0.9)<sup>[20]</sup>). Similarly, for [Yb(NCS)<sub>2</sub>(Ph<sub>2</sub>pz)(thf)<sub>4</sub>] the nonlinear SCN–Yb–NCS arrangement possibly results from ligand–ligand repulsion between the thiocyanates and the phenyl substituents on the pyrazolate. The plane of the pyrazolate ring is orientated more perpendicular than parallel (interplanar angle 77.8°) to the equatorial plane of the bipyramid (defined by Yb(1), O(4), O(4A), O(5), O(5A) and N<sub>i</sub>) thereby placing the phenyl groups in the vicinity of the thiocyanates. As a consequence, the thiocyanate ligands are pushed towards the gap between O(5) and O(5A) giving angles between axial N(1) and the equatorial atoms of less than 90° for O(5/5A) and greater than 90° for N<sub>i</sub> and O(4/4A) (Table 5). It should be noted however, that the two crystallographically independent [Yb(NCS)<sub>3</sub>(thf)<sub>4</sub>] molecules, for which steric factors should be less, also display nonlinear N–Yb–N angles (173.1(7) and 166.6(7)°),<sup>[9]</sup> albeit to a lesser degree, indicating that other influences may also be significant.

The Yb–N(thiocyanate) bond lengths for all three complexes lie within a narrow range of values (2.282(5)–2.302(3) Å) (Tables 3–5). This is remarkable given the about 0.11 Å change in the Yb<sup>3+</sup> ionic radii for coordination numbers six to eight<sup>[17]</sup> and the differences, both steric and electronic, of the A ligands. The Yb–N bond lengths are within the range (2.222(7)–2.314(5) Å) observed for [Yb(NCS)<sub>3</sub>(thf)<sub>4</sub>].<sup>[9]</sup> The Yb–O(OAr) bond length in **4** is shorter than the Yb–O(thf) bond (Table 3) as would be expected for an anionic oxygen, but it is also marginally shorter than the corresponding bonds in five coordinate [Yb(Odpp)<sub>3</sub>(thf)<sub>2</sub>]·THF (⟨Yb–O⟩ 2.078(9) Å).<sup>[29]</sup> Presumably, the presence of two further bulky Odpp ligands in the Yb(Odpp)<sub>3</sub> complex inhibits a closer contact between the

phenolate oxygen and the ytterbium atom in these structures. Furthermore, the Yb–O(OAr) distance is also shorter than that (2.083(5) Å) of [YbCl<sub>2</sub>(OAr)(thf)<sub>3</sub>] (OAr = OC<sub>6</sub>H<sub>2</sub>-2,6-*t*Bu<sub>2</sub>-4-Me),<sup>[36]</sup> consistent with the much bulkier aryloxy<sup>[20]</sup> in the chloro complex. There are minor variations in the ytterbium(III)–carbon bond lengths of **6** (Table 4) attributable to a slight ring tilt, with the longest Yb–C bond corresponding to the methyl-substituted carbon. However, the values are not unusual and subtraction of the Yb<sup>3+</sup> ionic radius<sup>[17]</sup> from ⟨Yb–C⟩ (2.63<sub>4</sub> Å) gives 1.65 Å, which is at the upper limit for cyclopentadienyllanthanoid(III) complexes.<sup>[37]</sup> The Yb–N(pyrazolate) bond lengths of **7** (Table 5) can be directly compared with other lanthanoid-η<sup>2</sup>-pyrazolate species by subtraction of the Yb<sup>3+</sup> ionic radius (0.985 Å).<sup>[17]</sup> This yields a value of 1.34 Å, which is within the range (1.31–1.38 Å) calculated for [Ln(Ph<sub>2</sub>pz)<sub>3</sub>L<sub>2</sub>] (L = thf, OPPh<sub>3</sub>) complexes,<sup>[31]</sup> although a considerably smaller value (1.26 Å) is obtained for the heteroleptic complex [Yb(C<sub>5</sub>Me<sub>5</sub>)<sub>2</sub>(Ph<sub>2</sub>Pz)].<sup>[38]</sup>

In **4** and **6** there is a pronounced lengthening of the Yb–O(thf) bond length for the THF ligand *trans* to the A ligand compared with those of the mutually *trans* THF ligands (Tables 3 and 4). The Yb–O(thf) bond lengths of [Yb(NCS)<sub>3</sub>(thf)<sub>4</sub>] display analogous behaviour.<sup>[9]</sup> In contrast, the Yb–O(thf) bond lengths (Table 5) of **7** show little difference. Overall, the average Yb–O(thf) bond lengths (2.30<sub>8</sub> (**4**), 2.36<sub>6</sub> (**6**), 2.39<sub>7</sub> (**7**) Å) vary in line with the respective coordination numbers. Subtraction of the appropriate ytterbium ionic radius<sup>[17]</sup> from the average Yb–O(thf) distances for all four thiocyanate complexes yields values (1.39, (**3**), 1.44 (**4**), 1.38 (**6**), 1.41 (**7**) Å) that, although somewhat larger than that (1.34(5) Å) derived from organolanthanoid-ether complexes,<sup>[39]</sup> agree well with the range derived from lanthanoid/chloride/thf complexes, for example, [LnCl<sub>3</sub>(thf)<sub>*n*</sub>] (1.39–1.44 Å).<sup>[7]</sup>

Summation of steric coordination numbers (ΣSt.CN)<sup>[20, 35]</sup> of the ligands for the complexes **3**–**7** gives values of 7.5 (**3**), 7.3 (**4**), 7.6 (**6**) and 8.3 (**7**) indicating that the Ph<sub>2</sub>Pz and Odpp complexes are the most and least crowded systems, respectively. Removal of one THF ligand from **7**, yielding an analogue of **4** and **6**, or addition of one THF ligand to **4**, providing an analogue of **3**, gives ΣSt.CN of 8.5 and 7.1. Both values lie outside the observed range suggesting that these compositions are less sterically comfortable (but see the microanalyses for **7**). The observed trend in the subtraction values for the Yb–O(thf) bond lengths does not follow that of the ΣSt.CN. In particular for **4**, even excluding the elongated *trans*-Yb–O(thf), the value (1.41 Å) is similar to that of **7**. In **4**, the THF ligands may be pushed away from the metal by the unexpectedly close approach (see above) of the Odpp ligand. In turn, the short Yb–O(OAr) bond possibly results from coordinative unsaturation, since a coordination number of six is considered low for the large lanthanoid cations (typically CN = 7–10).

The structures of [Yb(NCS)<sub>2</sub>A(thf)<sub>3</sub>] (A = Odpp, MeC<sub>5</sub>H<sub>4</sub>) are analogous to the related ytterbium–halide complexes [YbCl<sub>2</sub>(OC<sub>6</sub>H<sub>2</sub>-2,6-*t*Bu<sub>2</sub>-4-Me)(thf)<sub>3</sub>]<sup>[36]</sup> and [YbX<sub>2</sub>Cp(thf)<sub>3</sub>] (X = Cl or Br)<sup>[40]</sup> demonstrating isostructural replacement of a halide with a thiocyanate (pseudohalide). To our knowledge, there exists no halide equivalent of [Yb(NCS)<sub>2</sub>(Ph<sub>2</sub>pz)(thf)<sub>4</sub>],

which represents a rare example of a functionalised pyrazolatanthanoid complex (see also  $[\text{Yb}(\text{C}_5\text{Me}_5)_2(\text{Ph}_2\text{pz})]^{[38]}$ ).

**Ionic  $[\text{YbCl}_2(\text{thf})_3][\text{Yb}(\text{NCS})_4(\text{thf})_3]$  (8):** The structure of crystals grown from THF/light petroleum revealed discrete solvated seven coordinate tetrakis(thiocyanato)ytterbium anions  $[\text{Yb}(\text{NCS})_4(\text{thf})_3]^-$  (Figure 6a) and seven coordinate dichloroytterbium cations  $[\text{YbCl}_2(\text{thf})_3]^+$  (Figure 6b) rather than a monomer analogous to  $[\text{Yb}(\text{NCS})_3(\text{thf})_4]^{[9]}$ . The ytterbium atom (Yb(2)) and the oxygen O(4) atom of one THF ligand in the cation and the ytterbium atom (Yb(1)) and the oxygen O(1) atom of one THF ligand in the anion lie on crystallographic twofold axes. The crystallisation of an ionic species parallels  $\text{LnCl}_3$  structural chemistry, in which  $[\text{LnCl}_3(\text{thf})_{3.5}]$  ( $\text{Ln} = \text{Gd}, \text{Dy}, \text{Er}, \text{Tm}, \text{Y}$ ) are also ionic for example  $[\text{LnCl}_2(\text{thf})_5]^+[\text{LnCl}_4(\text{thf})_2]^-$ , and indeed contain a similar cation.<sup>[7]</sup> However, this structural type was not

observed for ytterbium, since  $\text{YbCl}_3$  instead crystallised from THF as monomeric  $[\text{YbCl}_3(\text{thf})_3]^{[7]}$ . Seven coordinate Yb in  $[\text{Yb}(\text{NCS})_4(\text{thf})_3]^-$  contrasts with six coordination in  $[\text{LnCl}_4(\text{thf})_2]^-$ .<sup>[7]</sup> Coordination of an extra THF ligand may be possible owing to the marginally smaller size of thiocyanate relative to chloride.<sup>[20]</sup> Similarly  $[\text{Yb}(\text{NCS})_3(\text{thf})_4]^{[9]}$  has four coordinated THF ligands compared with three in  $[\text{YbCl}_3(\text{thf})_3]^{[7]}$ . As was noted for the chlorides, relative solubilities may also influence the form of the crystalline phase.<sup>[7]</sup>

The geometry of the  $[\text{YbCl}_2(\text{thf})_3]^+$  cation is typical of the analogous cations with the larger lanthanoids<sup>[7]</sup> and is close to a regular pentagonal bipyramid (Table 6). The Yb–Cl and Yb–O bond lengths (Table 6) are marginally smaller than the corresponding values for the analogous erbium cation, consistent with the difference in the ionic radius between the respective metals.<sup>[17]</sup> Anionic lanthanoid thiocyanates of the type  $[\text{NR}_4]_{n-3}[\text{Ln}(\text{NCS})_n]$  are well known, typically with  $6 \leq n \leq 8$ .<sup>[41]</sup> Under certain conditions, however, mixed ligand  $[\text{Ln}(\text{NCS})_4(\text{OH}_2)_4]^-$  ( $\text{Ln} = \text{Nd}, \text{Eu}$ ) anions can be obtained.<sup>[42]</sup> Presumably a combination of the small  $\text{H}_2\text{O}$  ligands and the larger lanthanoids allows eight coordination in these cases. The four thiocyanates in the  $[\text{Yb}(\text{NCS})_4(\text{thf})_3]^-$  anion are disposed in an approximately equatorial arrangement. One THF ligand is in an axial position, but the other two THF ligands lie either side of the other pseudo-octahedral axial site. As a consequence of the uneven coordination on either side of the  $\text{Ln}(\text{NCS})_4$  unit, the thiocyanate ligands are displaced toward the least occupied space as revealed by *transoid* N–Yb–N angles  $155.6(6)$  and  $162.1(5)^\circ$ . The Yb–N bond lengths (Table 6) are at the high end of the range observed for seven coordinate  $[\text{Yb}(\text{NCS})_3(\text{thf})_4]^{[9]}$  whilst the Yb–O bond lengths (Table 6) lie between the extremes of those of the tris(thiocyanato)ytterbium complex.<sup>[9]</sup>

**Dimeric  $[\{\text{Yb}(\text{NCS})(\text{O}_2\text{CPh})_2(\text{thf})_2\}_2]$  (9):** The molecular structure of **9** is shown in Figure 7. The molecule is sited on a crystallographic inversion centre at the midpoint of the Yb(1)⋯Yb(1A) vector. Each

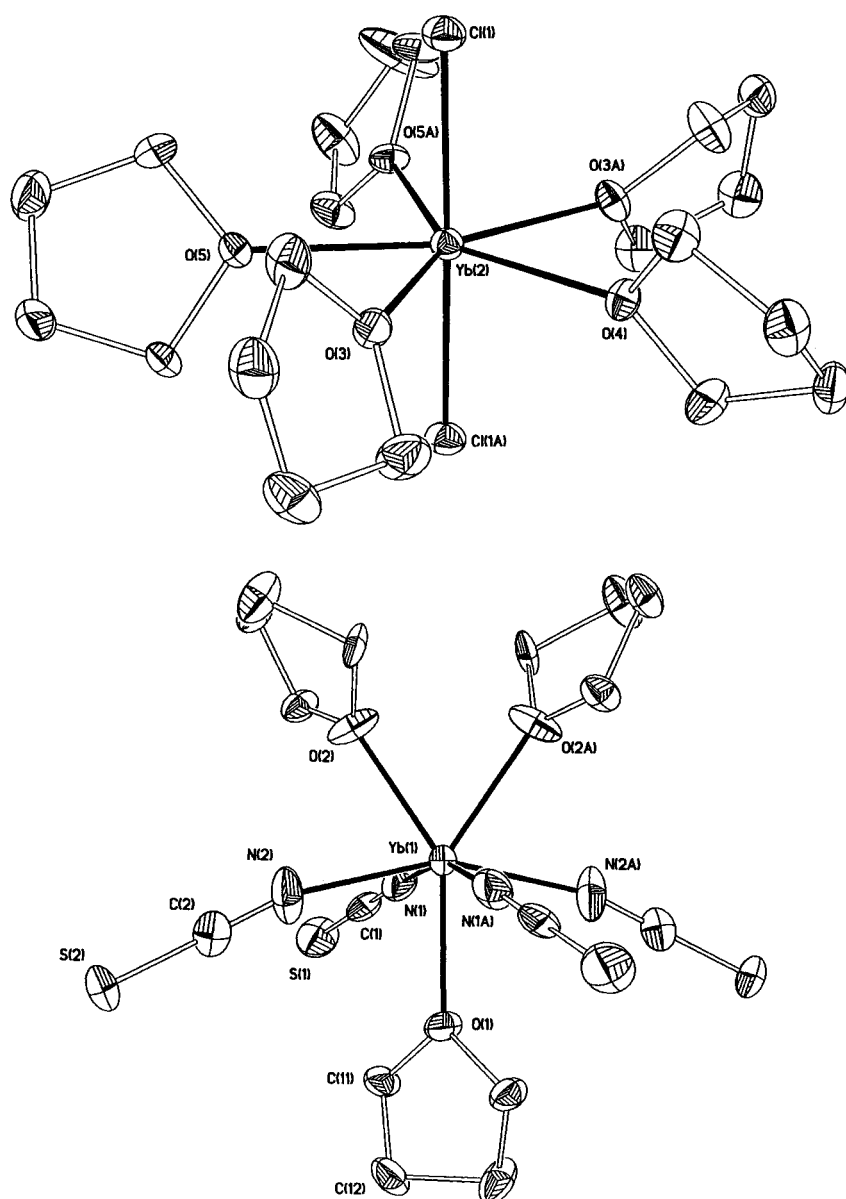


Figure 6. The X-ray structure of a)  $[\text{YbCl}_2(\text{thf})_3]^+$  and b)  $[\text{Yb}(\text{NCS})_4(\text{thf})_3]^-$  in **8**; 30% thermal ellipsoids are shown for the non-hydrogen atoms; hydrogen atoms have been omitted for clarity.

Table 6. Selected bond lengths [Å] and angles [°] for [YbCl<sub>2</sub>(thf)<sub>3</sub>]<sup>+</sup>[Yb(NCS)<sub>4</sub>(thf)<sub>3</sub>]<sup>-</sup> (**8**).

[YbCl <sub>2</sub> (thf) <sub>3</sub> ] <sup>+</sup>		[Yb(NCS) <sub>4</sub> (thf) <sub>3</sub> ] <sup>-</sup>	
Yb(2)–Cl(1)	2.533(2)	Yb(1)–N(1)	2.318(9)
Yb(2)–O(3)	2.355(4)	Yb(1)–N(2)	2.288(9)
Yb(2)–O(4)	2.339(4)	Yb(1)–O(1)	2.325(6)
Yb(2)–O(5)	2.364(3)	Yb(1)–O(2)	2.336(4)
Cl(1)–Yb(2)–Cl(1A) <sup>[a]</sup>	178.53(7)	N(1)–Yb(1)–N(1A) <sup>[b]</sup>	162.1(5)
Cl(1)–Yb(2)–O(3)	88.8(1)	N(2)–Yb(1)–N(2A) <sup>[b]</sup>	155.6(6)
Cl(1)–Yb(2)–O(4)	90.74(4)	N(1)–Yb(1)–N(2)	92.5(3)
Cl(1)–Yb(2)–O(5)	91.9(2)	N(1)–Yb(1)–N(2A) <sup>[b]</sup>	83.7(3)
Cl(1)–Yb(2)–O(3A) <sup>[a]</sup>	91.6(1)	N(1)–Yb(1)–O(1)	81.1(3)
Cl(1)–Yb(2)–O(5A) <sup>[a]</sup>	86.9(2)	N(1)–Yb(1)–O(2)	76.7(3)
O(3)–Yb(2)–O(3A) <sup>[a]</sup>	144.3(2)	N(1)–Yb(1)–O(2A) <sup>[b]</sup>	118.9(3)
O(3)–Yb(2)–O(4)	72.1(1)	N(2)–Yb(1)–O(1)	77.8(3)
O(3)–Yb(2)–O(5)	72.0(2)	N(2)–Yb(1)–O(2)	75.9(3)
O(3)–Yb(2)–O(5A) <sup>[a]</sup>	143.6(1)	N(2)–Yb(1)–O(2A) <sup>[b]</sup>	126.9(4)
O(4)–Yb(2)–O(5)	143.99(9)	O(1)–Yb(1)–O(2)	144.5(1)
O(5)–Yb(2)–O(5A) <sup>[a]</sup>	72.0(2)	O(2)–Yb(1)–O(2A) <sup>[b]</sup>	70.9(3)

[a] Symmetry transformations used to generate equivalent atoms:  $-x, -y + 1, z$ . [b] Symmetry transformations used to generate equivalent atoms:  $-x - 1, -y + 1, z$ .

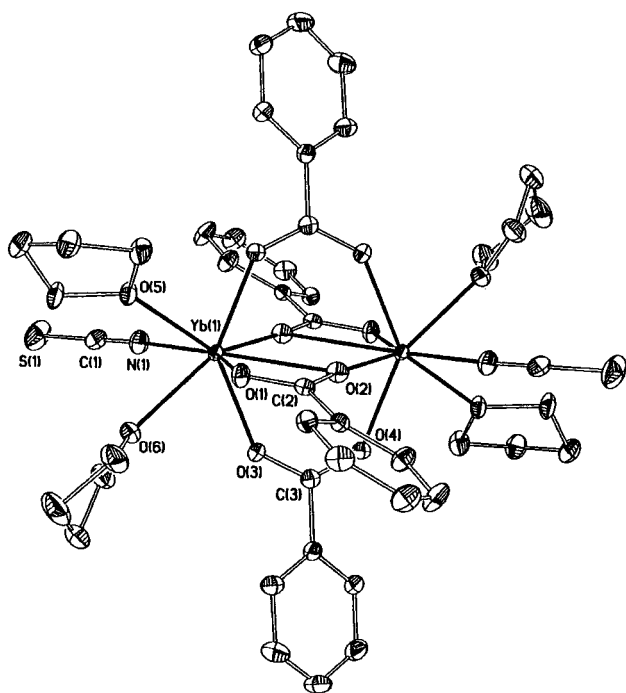


Figure 7. The X-ray structure of  $[[\text{Yb}(\text{NCS})(\mu\text{-O}_2\text{CPh})_2(\text{thf})_2]_2]$  (**9**); 50% thermal ellipsoids are shown for the non-hydrogen atoms; hydrogen atoms have been omitted for clarity.

ytterbium is surrounded by one thiocyanate, two THF ligands and four bridging benzoate groups. The carboxylates exhibit two different bonding modes, two being bridging bidentate and the other two being unsymmetrical bridging tridentate (chelated to one ytterbium and bonded through one oxygen to the other) giving an overall coordination number for each ytterbium atom of eight. Pairs of similar carboxylates in the central  $\{\text{Yb}(\mu\text{-OCO})_4\text{Yb}\}$  core of the dimer are approximately planar and orthogonal to each other in a “paddle wheel” arrangement. The geometry of each ytterbium atom approximates a bicapped trigonal prism with O(1), O(4A), O(5) and

N(1), O(2A), O(3) occupying the triangular vertices (interplanar angle  $8.9(1)^\circ$ ) and O(2) and O(6) as the capping atoms.

The Yb–N bond length in **9** (Table 7) is not significantly different from those of eight coordinate **6** or **7** (above) despite the significant difference in  $\nu(\text{CN})$  frequencies. The simple bridging bidentate benzoate group is bound to both ytterbium

Table 7. Selected bond lengths [Å] and angles [°] for  $[[\text{Yb}(\text{NCS})(\mu\text{-O}_2\text{CPh})_2(\text{thf})_2]_2]$  (**9**).

Yb(1)–N(1)	2.309(2)	Yb(1)–O(3)	2.259(2)
Yb(1)–O(1)	2.268(2)	Yb(1)–O(4A) <sup>[a]</sup>	2.255(2)
Yb(1)–O(2)	2.695(2)	Yb(1)–O(5)	2.385(2)
Yb(1)–O(2A) <sup>[a]</sup>	2.259(3)	Yb(1)–O(6)	2.433(3)
Yb(1)⋯Yb(1A) <sup>[a]</sup>	3.869(2)		
N(1)–Yb(1)–O(5)	79.58(8)	C(2)–O(1)–Yb(1)	103.7(2)
N(1)–Yb(1)–O(6)	75.90(8)	C(2)–O(2)–Yb(1A) <sup>[a]</sup>	174.1(2)
O(5)–Yb(1)–O(6)	72.89(7)	O(1)–Yb(1)–O(2)	51.63(7)
C(3)–O(3)–Yb(1)	139.4(2)	O(2)–Yb(1)–O(2A) <sup>[a]</sup>	77.67(7)
C(3)–O(4)–Yb(1A) <sup>[a]</sup>	133.7(2)	Yb(1)–O(2)–Yb(1A) <sup>[a]</sup>	102.33(7)

[a] Symmetry operations to generate equivalent atoms:  $-x - 1, -y + 1, -z + 1$ .

centres with near equivalent Yb(1)–O(3) and Yb(1A)–O(4) ( $\equiv$  Yb(1)–O(4A)) bond lengths (Table 7). Subtraction of the ionic radius<sup>[17]</sup> for eight coordinate Yb<sup>3+</sup> gives 1.274 and 1.270 Å, which are comparable to similarly derived values for eight coordinate  $[[\text{SmL}_2(\mu\text{-O}_2\text{CPh})_2]$  ( $\text{L} = \text{HBpz}_3$ , 1.22–1.30 Å,<sup>[33]</sup>  $\text{L} = \text{C}_5\text{Me}_5$ , 1.224, 1.238 Å<sup>[34]</sup>), but somewhat smaller than those for the chelating benzoate in  $[\text{Yb}(\text{HBpz}_3)_2(\text{O}_2\text{CPh})]$  (1.325–1.372 Å).<sup>[32]</sup> The high symmetry of the Yb(1)–O(3)–C(3)–O(4)–Yb(1A) linkage is clearly indicated by near identical C–Yb–O angles (Table 7). The other bridging benzoate group displays Yb(1)–O(1) and Yb(1A)–O(2) ( $\equiv$  Yb(1)–O(2A)) distances comparable to those above, but the C–Yb–O angles differ by almost  $70^\circ$ , with the C(2)–O(2)–Yb(1A) angle being near linear. As a consequence, O(2) is close enough to Yb(1) (Table 7) to be considered as bonding and hence this bridging benzoate is also chelated to Yb(1) (bridging tridentate coordination<sup>[43]</sup>). The geometry of chelation is highly unsymmetrical ( $\Delta(\text{Yb}–\text{O})$  0.427 Å); this is in contrast to, for example, recent observation of bridging tridentate carboxylate coordination in  $[[\text{Yb}(\text{C}_5\text{H}_5)_2(\text{O}_2\text{CMe})_2]$ , which displayed near equivalent Yb–O(chelate) bond lengths, but inequivalent bridging Yb–O lengths.<sup>[44]</sup> However, the symmetry of the chelate has been shown to depend upon ion size and steric factors in the series  $[[\text{Ln}(\text{C}_5\text{Me}_4\text{H})_2(\text{O}_2\text{CMe})_2]$   $\text{Ln} = \text{La}, \text{Sm}, \text{Y}$ .<sup>[45]</sup>

$[[\text{Yb}(\text{NCS})_2(\text{thf})_3]_2(\mu\text{-OC}(\text{Ph})_2\text{C}(\text{Ph})_2\text{O})] \cdot \text{THF}$  (**10**): The structure of the pinacolate complex **10** (Figure 8) shows a reductively generated 1,1,2,2-tetraphenylethane-1,2-diolate ligand bridging two ytterbium(III) centres. These have distorted octahedral coordination derived from one of the pinacolate oxygens, two *transoid* thiocyanates and three *mer*-THF ligands and are directly comparable with the ytterbium environment exhibited by the phenolate complex **4** (see above). Thus, the geometry is distorted octahedral with the mutually *transoid* thiocyanate and THF ligands displaced



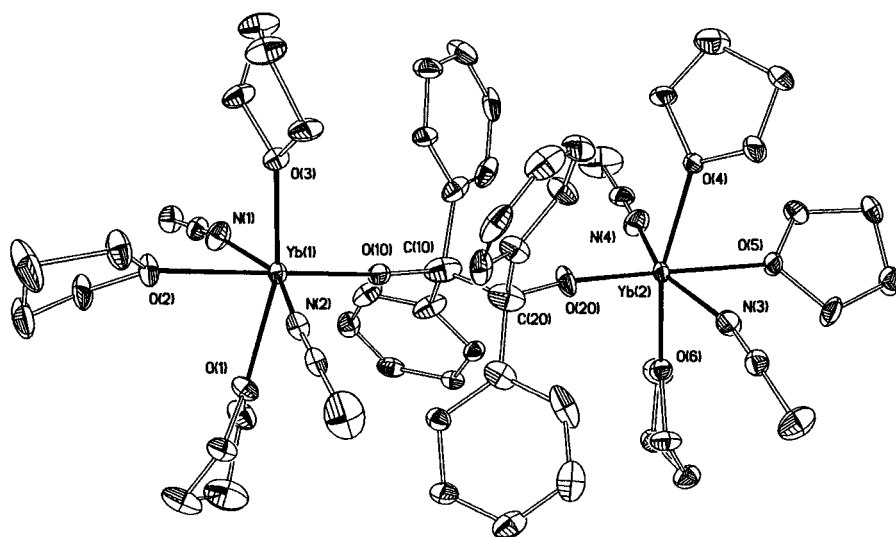


Figure 8. The X-ray structure of  $[(\text{Yb}(\text{NCS})_2(\text{thf})_3)_2(\mu\text{-OC}(\text{Ph})_2\text{C}(\text{Ph})_2\text{O})]\cdot\text{THF}$  (**10**); 30% thermal ellipsoids are shown for the non-hydrogen atoms; hydrogen atoms and the THF of solvation have been omitted for clarity.

towards the other THF, which in turn has a lengthened Yb–O bond length (Table 8) due to its *trans* disposition relative to the anionic alkoxo oxygen. The Yb–N and Yb–O(thf) bond lengths (Table 8) are marginally longer in **10** than in **4** (see above), suggestive of increased steric crowding in **10**. How-

Table 8. Selected bond lengths [ $\text{\AA}$ ] and angles [ $^\circ$ ] for  $[(\text{Yb}(\text{NCS})_2(\text{thf})_3)_2(\mu\text{-OC}(\text{Ph})_2\text{C}(\text{Ph})_2\text{O})]\cdot\text{THF}$  (**10**).

Yb(1)–N(1)	2.317(6)	Yb(1)–O(1)	2.302(5)
Yb(1)–N(2)	2.310(6)	Yb(1)–O(2)	2.383(5)
Yb(2)–N(3)	2.283(6)	Yb(1)–O(3)	2.297(5)
Yb(2)–N(4)	2.247(6)	Yb(2)–O(4)	2.309(5)
Yb(1)–O(10)	2.006(5)	Yb(2)–O(5)	2.365(5)
Yb(2)–O(20)	1.987(5)	Yb(2)–O(6)	2.302(4)
N(1)–Yb(1)–N(2)	159.9(2)	N(3)–Yb(2)–N(4)	159.8(2)
O(10)–Yb(1)–O(2)	178.2(2)	O(20)–Yb(2)–O(5)	176.8(2)
O(1)–Yb(1)–O(3)	161.1(2)	O(4)–Yb(2)–O(6)	161.1(2)
O(10)–Yb(1)–N(1)	98.0(2)	O(2)–Yb(1)–N(1)	80.2(2)
O(10)–Yb(1)–N(2)	101.0(2)	O(2)–Yb(1)–N(2)	80.7(2)
O(10)–Yb(1)–O(1)	97.8(2)	O(2)–Yb(1)–O(1)	81.9(2)
O(10)–Yb(1)–O(3)	100.5(2)	O(2)–Yb(1)–O(3)	80.0(2)
O(20)–Yb(2)–N(3)	97.6(3)	O(5)–Yb(2)–N(3)	79.2(2)
O(20)–Yb(2)–N(4)	102.5(3)	O(5)–Yb(2)–N(3)	80.6(2)
O(20)–Yb(2)–O(4)	100.3(2)	O(5)–Yb(2)–O(4)	79.4(2)
O(20)–Yb(2)–O(6)	98.1(2)	O(5)–Yb(2)–O(6)	82.5(2)

ever, in contrast, the Yb–O(OR) bond lengths in **10** (Table 8) are even shorter than the already unusually short Yb–O(OAr) bond length in **4**. Subtraction of the six coordinate  $\text{Yb}^{3+}$  ionic radius gives a value of 1.12  $\text{\AA}$ , much shorter than usual in bulky phenolates (1.26–1.32  $\text{\AA}$ )<sup>[21b, 29, 35a]</sup> and is at the low end for values of lanthanoid  $\text{Ph}_3\text{PO}$  complexes, which have the shortest Ln–O bond lengths of any O-donors.<sup>[46]</sup> The unique feature of **10** is the newly formed central C–C bond of the bridging 1,1,2,2-tetraphenylethane-1,2-dioxy ligand, which at 1.53(1)  $\text{\AA}$  is typical of a covalent C–C single bond. For the analogous  $[\text{SmA}_2(\mu\text{-pinacolate})(\text{L}_x)]$  complexes formed from reduction of fluorenone (see above) the C–C bond lengths are significantly longer

(e.g., 1.613(9)  $\text{\AA}$ ,  $\text{A} = \text{OC}_6\text{H}_2\text{-2,6-}t\text{Bu}_2\text{-4-Me}$ ,  $\text{L} = \text{Et}_2\text{O}$ )<sup>[26]</sup> indicative of stronger carbon bonding in **10**. With the normal central C–C bond in **10**, the stability to dissociation into ketyl radicals (see above) can be understood. The structure of **10** is the first of a lanthanoid(III) pinacolate with halide or pseudohalide coligands.

## Conclusion

The redox transmetalation reaction of ytterbium metal with mercuric thiocyanate provides a convenient source of  $[\text{Yb}(\text{NCS})_2(\text{thf})_2]$  (**1**), a new reducing reagent in lanthanoid

chemistry. Oxidation of **1** is facile and generates a diverse range of unique heteroleptic complexes of the type  $[\text{Yb}(\text{NCS})_2\text{A}(\text{thf})_n]$  or  $[\text{Yb}(\text{NCS})\text{A}_2(\text{thf})_n]$ , depending on the ligand “A”. Extensive characterisation, by single-crystal X-ray structure determination of these highly crystalline compounds reveal both similarities to lanthanoid halide structures as well as new structural prototypes. At this stage, it appears that the majority of oxidations of **1** proceed without rearrangement. Apart from intrinsic interest, the derived products may prove suitable for secondary functionalisation by replacement of thiocyanate. This would be of particular value in cases where the corresponding halides are currently inaccessible. Furthermore, the reaction of **1** with benzophenone indicates that  $\text{Yb}(\text{NCS})_2$  may have applications in organic synthesis.

## Experimental Section

All lanthanoid compounds described here are air and moisture sensitive. All manipulations were carried out under purified (BASF R3/11 oxygen removal catalyst and activated 4A molecular sieves) nitrogen or argon using standard Schlenk and drybox techniques. Solvents (THF, DME and light petroleum b.p. 60–70  $^\circ\text{C}$ ) were dried and deoxygenated by refluxing over blue sodium benzophenone ketyl under purified nitrogen. Tetraethyleneglycol dimethyl ether was added to the light petroleum to dissolve the ketyl. Elemental analyses (C,H,N) were performed by The Campbell Microanalytical Laboratory, Chemistry Department, University of Otago, Dunedin, New Zealand. Metal analyses were from EDTA titrations with xylenol orange indicator of buffered (hexamethylene tetraamine) aqueous solutions prepared by acid digestion of accurately weighed samples. IR spectra were obtained for Nujol mulls with a Perkin–Elmer 1600 FTIR instrument. The  $^{171}\text{Yb}$  NMR spectrum for compound **1** was recorded on a Bruker AM300 spectrometer. Data are reported relative to an external 0.15 M solution of  $\text{Yb}(\text{C}_5\text{Me}_5)_2$  in THF/10%  $\text{C}_6\text{D}_6$ .<sup>[16]</sup> UV/visible/near IR spectra were obtained for solutions in a 1 mm quartz cell by using a Carey 17 spectrophotometer. Ytterbium metal powder was obtained from Rhône Poulenc. Anhydrous mercury(II) thiocyanate (May and Baker), 2,6-diphenylphenol, hexachloroethane and benzophenone (Aldrich) were used as received. Other reagents,  $\text{Hg}(\text{C}_6\text{F}_5)_2$ ,<sup>[47]</sup>  $\text{Ti}(\text{C}_5\text{H}_5)_2$ ,<sup>[48]</sup>  $\text{Ti}(\text{C}_5\text{H}_5\text{Me})_2$ ,<sup>[48]</sup>  $\text{Ti}(\text{Ph}_2\text{pz})_2$ <sup>[31b]</sup> and  $\text{Ti}(\text{O}_2\text{CPh})_2$ <sup>[49]</sup> were prepared by the reported methods.

**$[\text{Yb}(\text{NCS})_2(\text{thf})_2]$  (**1**):** Ytterbium metal (2.73 g, 15.8 mmol) and  $\text{Hg}(\text{SCN})_2$  (2.32 g, 7.3 mmol) were stirred in THF (20 mL) for 24 h. The reaction

mixture was filtered through a Celite pad, and the pad was washed with THF (3 × 10 mL). The combined yellow filtrate and washings were evaporated to initially a yellow crystalline material, which when further dried under vacuum with gentle heating gave red microcrystalline **1**. Yield 2.98 g, 94%; IR (Nujol):  $\tilde{\nu}$  = 2085 (vs), 2044 (m), 1979 (sh), 1440 (w), 1295 (w), 1244 (w), 1177 (w), 1027 (s), 949 (w), 917 (w), 876 (s), 769 (w), 722 cm<sup>-1</sup> (m); <sup>171</sup>Yb{<sup>1</sup>H} NMR (52.1 MHz, THF, 298 K):  $\delta$  = 340, brs ( $\Delta\nu_{1/2}$  90 Hz); visible/near IR (THF):  $\lambda_{\text{max}}$  ( $\epsilon$ ) = 408 nm (778 dm<sup>3</sup> mol<sup>-1</sup> cm<sup>-1</sup>); elemental analysis calcd (%) for C<sub>10</sub>H<sub>16</sub>N<sub>2</sub>O<sub>2</sub>S<sub>2</sub>Yb (433.41): Yb 39.93; found Yb 40.28.

**[Yb(NCS)<sub>2</sub>(dme)<sub>3</sub>] (2)**: Recrystallisation of solid **1**, prepared as above from ytterbium metal (2.60 g, 15.0 mmol) and Hg(SCN)<sub>2</sub> (3.20 g, 10.1 mmol), from DME gave large yellow blocks of **2**. Yield 2.21 g, 40%; IR (Nujol):  $\tilde{\nu}$  = 2099 (m), 2057 (vs), 1273 (w), 1245 (w), 1189 (w), 1156 (w), 1113 (m), 1059 (s), 1026 (m), 967 (w), 863 (m), 855 (m), 836 (w), 777 (w), 722 cm<sup>-1</sup> (w); elemental analysis calcd (%) for C<sub>14</sub>H<sub>30</sub>N<sub>2</sub>O<sub>6</sub>S<sub>2</sub>Yb (559.57): C 30.05, H 5.40, N 5.01; found C 29.81, H 5.28, N 5.02.

**Oxidation reactions**: Amounts of reagents, reaction conditions and product yields are listed in Table 2. In general, the reagents were stirred under argon in THF at room temperature for the time specified. The reaction mixtures were then filtered and the products were isolated as described below.

**[Yb(NCS)<sub>3</sub>(thf)<sub>4</sub>] (3)**: The colourless filtrate was reduced in volume to about 10 mL and light petroleum (10 mL) was added until incipient crystallisation. After standing overnight, colourless crystals of **3** formed. IR (Nujol):  $\tilde{\nu}$  = 2038 (vs), 1299 (w), 1172 (w), 1075 (w), 1039 (w), 1010 (m), 956 (w), 919 (w), 841 (m), 722 cm<sup>-1</sup> (m); this is in satisfactory agreement with reported data:<sup>[9]</sup> visible/near IR (THF):  $\lambda_{\text{max}}$  ( $\epsilon$ ) = 414 (86), 925 (5), 976 nm (14 dm<sup>3</sup> mol<sup>-1</sup> cm<sup>-1</sup>); elemental analysis calcd (%) for C<sub>19</sub>H<sub>32</sub>N<sub>3</sub>O<sub>4</sub>S<sub>3</sub>Yb (635.70): Yb 27.22; found Yb 27.84.

**[Yb(NCS)<sub>2</sub>(Odpp)(thf)<sub>3</sub>] (4)**: The yellow filtrate was evaporated to 10 mL and large bright yellow blocks of **4** deposited after standing overnight. IR (Nujol):  $\tilde{\nu}$  = 2031 (sbr), 1599 (w), 1578 (w), 1416 (m), 1311 (w), 1286 (m), 1268 (m), 1178 (w), 1150 (w), 1085 (w), 1074 (m), 1040 (w), 1012 (s), 954 (w), 918 (w), 856 (s), 772 (m), 753 (s), 712 cm<sup>-1</sup> (s); elemental analysis calcd (%) for C<sub>32</sub>H<sub>37</sub>N<sub>2</sub>O<sub>4</sub>S<sub>2</sub>Yb (750.82): C 51.19, H 4.97, N 3.73; found C 51.18, H 5.25, N 3.58. Stirring of **1** (0.43 g, 1.0 mmol) and HODpp (0.26 g, 1.0 mmol) in THF (30 mL) at room temperature for several days followed by removal of the solvent gave a mixture of the starting materials and no **4** (IR identification).

**[Yb(NCS)<sub>2</sub>(C<sub>5</sub>H<sub>5</sub>)(thf)<sub>3</sub>] (5)**: Concentration of the orange filtrate to 15 mL and cooling to -20 °C gave orange crystals of **5**. IR (Nujol):  $\tilde{\nu}$  = 2045 (vs), 1296 (w), 1254 (w), 1171 (w), 1129 (sh), 1014 (s), 922 (w), 861 (s), 795 (s), 776 (s), 722 cm<sup>-1</sup> (w); visible/near IR (THF):  $\lambda_{\text{max}}$  ( $\epsilon$ ) 448 (70), 926 (7), 982 nm (59 dm<sup>3</sup> mol<sup>-1</sup> cm<sup>-1</sup>); elemental analysis calcd (%) for C<sub>19</sub>H<sub>29</sub>N<sub>2</sub>O<sub>3</sub>S<sub>2</sub>Yb (570.61): C 39.99, H 5.12, N 4.91, Yb 30.33; found C 38.67, H 5.13, N 5.25, Yb 30.23.

**[Yb(NCS)<sub>2</sub>(C<sub>5</sub>H<sub>4</sub>Me)(thf)<sub>3</sub>] (6)**: Orange crystals of **6** were isolated as for **5** above. IR (Nujol):  $\tilde{\nu}$  = 2045 (vs), 1342 (w), 1295 (w), 1242 (w), 1174 (m), 1030 (s), 1013 (s), 980 (m), 952 (w), 921 (m), 858 (s), 835 (s), 777 (s), 723 cm<sup>-1</sup> (w); elemental analysis calcd (%) for C<sub>20</sub>H<sub>31</sub>N<sub>2</sub>O<sub>3</sub>S<sub>2</sub>Yb (584.64): Yb 29.60; found Yb 30.29.

**[Yb(NCS)<sub>2</sub>(Ph<sub>2</sub>pz)(thf)<sub>4</sub>] (7)**: The pale yellow filtrate was reduced in volume to 20 mL and cooled to -20 °C; this resulted in the deposition of large pale yellow crystals of **7**. IR (Nujol):  $\tilde{\nu}$  = 2048 (vs), 1604 (m), 1311 (w), 1297 (w), 1172 (w), 1154 (w), 1064 (m), 1023 (s), 972 (m), 918 (m), 869 (s), 808 (w), 770 (s), 722 (m), 703 (m), 688 cm<sup>-1</sup> (w); elemental analysis calcd (%) for C<sub>33</sub>H<sub>43</sub>N<sub>4</sub>O<sub>4</sub>S<sub>2</sub>Yb (796.90): C 49.74, H 5.44, N 7.03, Yb 21.71; found C 47.63, H 5.18, N 8.01, Yb 22.32 {elemental analysis calcd (%) for [Yb(NCS)<sub>2</sub>(Ph<sub>2</sub>pz)(thf)<sub>3</sub>] C<sub>29</sub>H<sub>35</sub>N<sub>4</sub>O<sub>3</sub>S<sub>2</sub>Yb (724.79): C 48.06, H 4.87, N 7.73, Yb 23.87}.

**[YbCl<sub>2</sub>(thf)<sub>3</sub>][Yb(NCS)<sub>4</sub>(thf)<sub>3</sub>] (8)**: The near colourless solution was evaporated to 20 mL and light petroleum (20 mL) was added causing formation of a colourless oil. Cooling to -20 °C gave **8** as a white solid. IR (Nujol):  $\tilde{\nu}$  = 2048 (vs), 1604 (m), 1311 (w), 1297 (w), 1172 (w), 1154 (w), 1064 (m), 1023 (s), 972 (m), 918 (m), 869 (s), 808 (w), 770 (s), 722 (m), 703 (m), 688 cm<sup>-1</sup> (w); elemental analysis calcd (%) for C<sub>36</sub>H<sub>64</sub>Cl<sub>2</sub>N<sub>4</sub>O<sub>8</sub>S<sub>4</sub>Yb<sub>2</sub> (1226.16): C 35.26, H 5.26, N 4.57; found C 34.92, H 5.37, N, 4.52. Single crystals were grown from THF/light petroleum at room temperature.

**Reaction of 1 and (benzoato)thallium(0)**: The pale yellow filtrate was evaporated to 20 mL. After addition of light petroleum (20 mL) and standing for several days, small colourless crystals of [[Yb(O<sub>2</sub>CPh)<sub>2</sub>(NCS)(thf)<sub>2</sub>]<sub>2</sub>] (**9**) were deposited. IR (Nujol):  $\tilde{\nu}$  = 2062 (vs), 1612 (s br), 1571 (s), 1496 (m), 1415 (vs), 1308 (w), 1173 (w), 1156 (w), 1071 (w), 1029 (s), 978 (w), 954 (w), 924 (m), 874 (s), 735 (s), 718 (s), 681 (m), 668 cm<sup>-1</sup> (m); elemental analysis calcd (%) for C<sub>46</sub>H<sub>52</sub>N<sub>2</sub>O<sub>12</sub>S<sub>2</sub>Yb<sub>2</sub> (1235.13): C 44.73, H 4.24, N 2.27; found C 41.81, H 4.01, N 2.40. From a separate preparation, cooling to -20 °C of the supernatant solution obtained after the first crystallisation, gave a mixture of some large block-shaped colourless crystals of **3** and a white powder. X-ray analysis of

Table 9. Crystal and refinement parameters.<sup>[a]</sup>

	<b>2</b>	<b>4</b> <sup>[b]</sup>	<b>6</b>	<b>7</b>	<b>8</b> <sup>[c]</sup>	<b>9</b>	<b>10</b>
formula	C <sub>14</sub> H <sub>30</sub> N <sub>2</sub> O <sub>6</sub> S <sub>2</sub> Yb	C <sub>32</sub> H <sub>37</sub> N <sub>2</sub> O <sub>4</sub> S <sub>2</sub> Yb	C <sub>20</sub> H <sub>31</sub> N <sub>2</sub> O <sub>3</sub> S <sub>2</sub> Yb	C <sub>33</sub> H <sub>43</sub> N <sub>4</sub> O <sub>4</sub> S <sub>2</sub> Yb	C <sub>36</sub> H <sub>64</sub> Cl <sub>2</sub> N <sub>4</sub> O <sub>8</sub> S <sub>4</sub> Yb <sub>2</sub>	C <sub>46</sub> H <sub>52</sub> N <sub>2</sub> O <sub>12</sub> S <sub>2</sub> Yb <sub>2</sub>	C <sub>38</sub> H <sub>76</sub> N <sub>4</sub> O <sub>9</sub> S <sub>4</sub> Yb <sub>2</sub>
<i>M<sub>r</sub></i>	559.56	750.80	584.63	796.87	1226.16	1235.13	1447.59
crystal system	monoclinic	monoclinic	monoclinic	orthorhombic	orthorhombic	triclinic	orthorhombic
space group	C2/c (No. 9)	P2 <sub>1</sub> /n (No.14)	P2 <sub>1</sub> /n (No.14)	Pbcn (No. 60)	P2 <sub>1</sub> 2 <sub>1</sub> 2 (No. 18)	P $\bar{1}$ (No. 2)	Pca2 <sub>1</sub> (No. 29)
<i>a</i> [Å]	20.9843(4)	11.5084(2)	10.5385(2)	9.8472(3)	11.6369(3)	9.8760(2)	17.1434(2)
<i>b</i> [Å]	8.8157(1)	14.0326(2)	15.1280(2)	19.5232(6)	17.8814(3)	11.1612(2)	17.7493(2)
<i>c</i> [Å]	14.7091(2)	20.1521(3)	14.4240(3)	17.8814(4)	11.5689(3)	12.0151(2)	20.3774(3)
$\alpha$ [°]						99.771(1)	
$\beta$ [°]	128.133(1)	92.778(1)	90.459(1)			113.430(1)	
$\gamma$ [°]						94.414(1)	
<i>V</i> [Å <sup>3</sup> ]	2140.3(7)	3250.6(11)	2299.5(8)	3457.6(12)	2407.3(8)	1182.2(4)	6201(2)
<i>Z</i>	4	4	4	4	2	1 (dimer)	4
$\rho_{\text{calcd}}$ [g cm <sup>-3</sup> ]	1.737	1.534	1.689	1.531	1.692	1.735	1.555
$\mu$ (MoK $\alpha$ ) [mm <sup>-1</sup> ]	4.593	3.042	4.271	2.867	4.194	4.082	3.186
crystal size	0.18 × 0.18 × 0.23	0.25 × 0.25 × 0.25	0.13 × 0.25 × 0.25	0.13 × 0.20 × 0.20	0.05 × 0.10 × 0.30	0.10 × 0.10 × 0.13	0.23 × 0.25 × 0.30
<i>F</i> (000)	1112	1508	1164	1612	1220	610	2925
2 $\theta_{\text{max}}$ [°]	60.1	55.7	55.7	60.1	55.8	60.1	54.6
<i>N</i> ( <i>R</i> <sub>int</sub> )	3105 (0.039)	7730 (0.034)	5206 (0.041)	4864 (0.091)	5746 (0.081)	6345 (0.027)	15384 (0.072)
<i>N</i> <sub>o</sub>	2918	6177	4678	3339	4225	5991	13321
absorption correction	0.933, 1.11 <sup>[c]</sup>	0.603, 0.691 <sup>[c]</sup>	0.546, 0.594 <sup>[c]</sup>	0.962, 1.03 <sup>[c]</sup>	0.436, 0.809 <sup>[d]</sup>	0.627, 0.670 <sup>[e]</sup>	N/A
<i>R</i> / <i>R</i> <sub>w</sub> [ <i>I</i> > 2 $\sigma$ ( <i>I</i> )]	0.026/0.063	0.042/0.098	0.032/0.066	0.054/0.056	0.050/0.068	0.023/0.050	0.038/0.091
<i>R</i> / <i>R</i> <sub>w</sub> (all data)	0.030/0.064	0.055/0.102	0.038/0.068	0.115/0.064	0.087/0.074	0.026/0.051	0.054/0.124
goodness of fit	1.114	1.291	1.173	1.184	1.027	1.078	1.212
$\delta\epsilon_{\text{min,max}}$ [e Å <sup>-3</sup> ]	-2.238, 1.876	-1.165, 1.933	-1.566, 1.149	-1.701, 0.669	-2.454, 1.964	-2.086, 1.098	-2.452, 1.072

[a] Measured at 123 K unless otherwise indicated. [b] Measured at 173 K. [c] Empirical (*A*\*<sub>min,max</sub>). [d] Face-indexed gaussian (*T*\*<sub>min,max</sub>). [e] Refined as a racemic twin.

the crystals gave the following cell constants ( $T=123(1)$  K):  $a=12.040(1)$ ,  $b=17.011(4)$ ,  $c=25.347(3)$  Å;  $\beta=90.17(1)^\circ$ ;  $V=3184$  Å<sup>3</sup>, which are close to the reported room-temperature data.<sup>[9]</sup>

**[{Yb(NCS)<sub>2</sub>(thf)<sub>2</sub>(OC(Ph)<sub>2</sub>C(Ph)<sub>2</sub>O)}]·THF (10):** After completion of the reaction, the mixture was heated giving a red solution, which was then filtered and allowed to slowly cool to room temperature. Large colourless crystals of **10** were deposited. IR (Nujol):  $\tilde{\nu}=2039$  (vs), 1310 (w), 1296 (w), 1162 (w), 1101 (s), 1070 (s), 1033 (w), 1010 (s), 955 (w), 915 (w), 855 (s), 765 (m), 745 (m), 722 (w), 703 (m), 676 cm<sup>-1</sup> (m); visible/near IR (THF):  $\lambda_{\text{max}}$  ( $\epsilon$ ) 929 (3), 978 nm (10 dm<sup>3</sup> mol<sup>-1</sup> cm<sup>-1</sup>); elemental analysis calcd (%) for C<sub>38</sub>H<sub>76</sub>N<sub>4</sub>O<sub>9</sub>S<sub>4</sub>Yb<sub>2</sub> (1447.59): C 48.12, H 5.29, N 3.87; found C 47.76, H 5.22, N 3.94.

**X-ray Crystallography:** Data for the crystallographic structure determination of compounds **2**, **4** and **6–10** are given in Table 9. Crystals were mounted in an inert atmosphere under viscous oil onto a glass fibre. Low-temperature (~123 K) data were collected on an Enraf–Nonius CCD area-detector diffractometer (MoK $\alpha$  radiation,  $\lambda$  0.71073 Å, frames comprised 1.0° increments in  $\phi$  and  $\omega$  yielding a sphere of data) with proprietary software (Nonius B.V., 1998). Corrections for absorption (face-indexed gaussian or empirical<sup>[50]</sup>) were applied as indicated. Each data set was merged ( $R_{\text{int}}$  as quoted) to  $N$  unique reflections; the structures were solved by conventional methods and refined with anisotropic thermal parameter forms for the non-hydrogen atoms by full-matrix least-squares on all  $F^2$  data by using SHELX 97 software package.<sup>[51]</sup> Hydrogen atoms were included in calculated positions and allowed to ride on the parent carbon atom with isotropic thermal parameters. Crystallographic data (excluding structure factors) for the structures reported in this paper have been deposited with the Cambridge Crystallographic Data Centre as supplementary publication nos. CCDC-150805 to CCDC-150811. Copies of the data can be obtained free of charge on application to CCDC, 12 Union Road, Cambridge CB2 1EZ, UK (fax: (+44)1223-336-033; e-mail: deposit@ccdc.cam.ac.uk).

## Acknowledgement

We are grateful to the Australian Research Council for financial support.

- [1] a) F. T. Edelmann in *Comprehensive Organometallic Chemistry II* (Eds. G. Wilkinson, F. G. A. Stone, E. W. Abel), Pergamon, Oxford, **1995**, Chapter 2; b) M. N. Bochkarev, L. N. Zharkov, G. S. Kalinina, *Organoderivatives of the Rare Earth Elements*, Kluwer, Dordrecht, **1995**; c) H. Schumann, J. A. Meese-Marktscheffel, L. Esser, *Chem. Rev.* **1995**, 95, 865.
- [2] a) G. A. Molander, C. R. Harris, *Chem. Rev.* **1996**, 96, 307; b) G. A. Molander, *Chem. Rev.* **1992**, 92, 29; c) T. Imamoto, *Lanthanides in Organic Synthesis*, Academic Press, London, **1994**; d) K. Mashima, T. Oshiki, K. Tani, *J. Org. Chem.* **1998**, 63, 7114; e) J. Collin, N. Giuseppone, F. Machrouhi, J.-L. Namey, F. Nief, *Tetrahedron Lett.* **1999**, 40, 3161; f) J. Collin, N. Giuseppone, P. Van de Weghe, *Coord. Chem. Rev.* **1998**, 178–180, 117.
- [3] F. A. Cotton, G. Wilkinson, *Advanced Inorganic Chemistry*, 5th ed., Wiley-Interscience, **1988**, Chapter 20.
- [4] D. J. Duncalf, P. B. Hitchcock, G. A. Lawless, *Chem. Commun.* **1996**, 269.
- [5] W. J. Evans, I. Bloom, J. W. Grate, L. A. Hughes, W. E. Hunter, J. L. Atwood, *Inorg. Chem.* **1985**, 24, 4620.
- [6] G. Lin, W.-T. Wong, *J. Organomet. Chem.* **1996**, 522, 271.
- [7] G. B. Deacon, T. Feng, P. C. Junk, B. W. Skelton, A. N. Sobolev, A. H. White, *Aust. J. Chem.* **1998**, 51, 75.
- [8] J. H. Melman, M. Fitzgerald, D. Freedman, T. J. Emge, J. G. Brennan, *J. Am. Chem. Soc.* **1999**, 121, 10247.
- [9] G. Depaoli, P. Ganis, P. L. Zanonato, *Polyhedron* **1993**, 12, 1933.
- [10] C. Wickleder, personal communication.
- [11] a) F. Benetollo, G. Bombiere, L. M. Vallarino, *Polyhedron* **1994**, 13, 573; b) S. M. Bowen, E. N. Duesler, R. T. Paine, *Inorg. Chim. Acta* **1984**, 84, 221; c) R. G. Lawrence, C. J. Jones, R. A. Kresinski, *Polyhedron* **1996**, 15, 2011; d) T. Labahn, A. Mandel, J. Magull, *Z. Anorg. Allg. Chem.* **1999**, 625, 1273.
- [12] F. Calderazzo, R. Pappalardo, S. Losi, *J. Inorg. Nucl. Chem.* **1966**, 28, 987.
- [13] A. H. Norbury, *Adv. Inorg. Chem. Radiochem.* **1975**, 77, 231.
- [14] G. B. Deacon, A. J. Koplick, T. D. Tuong, *Aust. J. Chem.* **1984**, 37, 517, and references therein.
- [15] S. P. Constantine, G. M. De Lima, P. B. Hitchcock, J. M. Keates, G. A. Lawless, *Chem. Commun.* **1996**, 2421.
- [16] A. G. Advent, M. A. Edelman, M. F. Lappert, G. A. Lawless, *J. Am. Chem. Soc.* **1989**, 111, 3423.
- [17] R. D. Shannon, *Acta Crystallogr. Sect. A* **1976**, 32, 751.
- [18] a) W. J. Evans, R. N. R. Broomhall-Dillard, J. W. Ziller, *Polyhedron* **1998**, 17, 3370; b) M. Håkansson, M. Vestergren, B. Gustafsson, G. Hilmersson, *Angew. Chem.* **1999**, 111, 2336; *Angew. Chem. Int. Ed.* **1999**, 38, 2199; c) T. Gröb, G. Seybert, W. Massa, K. Dehnicke, *Z. Anorg. Allg. Chem.* **1999**, 625, 1897.
- [19] a) M. N. Bochkarev, I. L. Fedushkin, A. A. Fagin, T. V. Petrovskaya, J. W. Ziller, W. J. Evans, *Angew. Chem.* **1997**, 109, 123; *Angew. Chem. Int. Ed. Engl.* **1997**, 36, 133; b) T. Gröb, G. Seybert, W. Massa, K. Dehnicke, *Z. Anorg. Allg. Chem.* **2000**, 626, 349.
- [20] J. Marçalo, P. De Matos, *Polyhedron* **1989**, 8, 2431.
- [21] a) G. B. Deacon, P. B. Hitchcock, S. A. Holmes, M. F. Lappert, P. MacKinnon, R. H. Newnham, *J. Chem. Soc. Chem. Commun.* **1989**, 935; b) G. B. Deacon, T. Feng, P. MacKinnon, R. H. Newnham, S. Nickel, B. W. Skelton, A. H. White, *Aust. J. Chem.* **1993**, 46, 387; c) J. R. van den Hende, P. B. Hitchcock, S. A. Holmes, M. F. Lappert, *J. Chem. Soc. Dalton Trans.* **1995**, 1435.
- [22] G. B. Deacon, G. D. Fallon, C. M. Forsyth, H. Schumann, R. Weimann, *Chem. Ber.* **1997**, 130, 409.
- [23] V. Chebolu, R. R. Whittle, A. Sen, *Inorg. Chem.* **1985**, 24, 3082.
- [24] G. Depaoli, P. Ganis, P. L. Zanonato, G. Valle, *Polyhedron* **1993**, 12, 671.
- [25] A. P. Purdy, C. F. George, *Main Group Chem.* **1996**, 1, 229.
- [26] Z. Hou, A. Fujita, Y. Zhang, T. Miyano, H. Yamazaki, Y. Wakatsuki, *J. Am. Chem. Soc.* **1998**, 120, 754.
- [27] W. Clegg, C. Eaborn, K. Izod, P. O'Shaughnessy, J. D. Smith, *Angew. Chem.* **1997**, 109, 2925; *Angew. Chem. Int. Ed. Engl.* **1997**, 36, 2815.
- [28] W. J. Evans, M. A. Hozbor, *J. Organomet. Chem.* **1987**, 326, 299.
- [29] G. B. Deacon, S. Nickel, P. MacKinnon, E. R. T. Tiekink, *Aust. J. Chem.* **1990**, 43, 1245.
- [30] J. E. Cosgriff, G. B. Deacon, *Angew. Chem.* **1998**, 110, 298; *Angew. Chem. Int. Ed.* **1998**, 37, 286.
- [31] a) J. E. Cosgriff, G. B. Deacon, B. M. Gatehouse, *Aust. J. Chem.* **1993**, 46, 1881; b) G. B. Deacon, E. E. Delbridge, B. W. Skelton, A. H. White, *Eur. J. Inorg. Chem.* **1998**, 543; **1999**, 751; c) J. E. Cosgriff, G. B. Deacon, G. D. Fallon, B. M. Gatehouse, H. Schumann, R. Weimann, *Chem. Ber.* **1996**, 129, 953.
- [32] M. A. J. Moss, C. J. Jones, *J. Chem. Soc. Dalton Trans.* **1990**, 581.
- [33] D. L. Reger, S. J. Knox, J. A. Lindeman, L. Lebioda, *Inorg. Chem.* **1990**, 29, 417.
- [34] W. J. Evans, C. A. Seibel, J. W. Ziller, R. J. Doedens, *Organometallics* **1998**, 17, 2103.
- [35] a) G. B. Deacon, T. Feng, B. W. Skelton, A. H. White, *Aust. J. Chem.* **1995**, 48, 741; b) Calculated from cone-angle factors in C. T. Abrahams, Ph.D. Thesis, Monash University, **1996**.
- [36] Y. Yao, Q. Shen, J. Sun, *Polyhedron* **1998**, 17, 519.
- [37] a) K. R. Raymond, C. W. Eigenbrot, *Acc. Chem. Res.* **1980**, 13, 276; b) S. C. Sockwell, T. P. Hanusa, *Inorg. Chem.* **1990**, 29, 76.
- [38] G. B. Deacon, E. E. Delbridge, G. D. Fallon, C. Jones, D. E. Hibbs, M. B. Hursthouse, B. W. Skelton, A. H. White, *Organometallics* **2000**, 19, 1713.
- [39] G. B. Deacon, P. I. MacKinnon, T. W. Hambley, J. C. Taylor, *J. Organomet. Chem.* **1983**, 259, 91.
- [40] G. B. Deacon, G. D. Fallon, D. L. Wilkinson, *J. Organomet. Chem.* **1985**, 293, 45.
- [41] a) J. L. Martin, L. C. Thompson, L. J. Radonovich, M. D. Glick, *J. Am. Chem. Soc.* **1968**, 90, 4493; b) H. Arai, Y. Suzuki, N. Matsumura, T. Takeuchi, A. Ouchi, *Bull. Chem. Soc. Jpn.* **1989**, 62, 2530; c) Y. Tateyama, Y. Kuniyasu, Y. Suzuki, A. Ouchi, *Bull. Chem. Soc. Jpn.* **1988**, 61, 2805; d) F. Matsumoto, T. Takeuchi, A. Ouchi, *Bull. Chem. Soc. Jpn.* **1989**, 62, 2078; e) F. Matsumoto, N. Matsumura, A. Ouchi, *Bull. Chem. Soc. Jpn.* **1989**, 62, 1809; f) N. Matsumura, T. Takeuchi, A. Ouchi, *Bull. Chem. Soc. Jpn.* **1990**, 63, 620.

- [42] A. Ouchi, *Bull. Chem. Soc. Jpn.* **1989**, 62, 2431.
- [43] A. Ouchi, Y. Suzuki, Y. Ohki, Y. Koizumi, *Coord. Chem. Rev.* **1988**, 92, 29.
- [44] G. B. Deacon, G. D. Fallon, A. Rabinovich, B. W. Skelton, A. H. White, *J. Organomet. Chem.* **1995**, 501, 23.
- [45] H. Schumann, K. Zietzke, R. Wiemann, *Eur. J. Solid State Inorg. Chem.* **1996**, 33, 121.
- [46] a) G. B. Deacon, G. D. Fallon, C. M. Forsyth, B. M. Gatehouse, P. C. Junk, A. Philosofo, P. A. White, *J. Organomet. Chem.* **1998**, 565, 201;  
b) G. B. Deacon, C. M. Forsyth, B. M. Gatehouse, A. Philosofo, B. W. Skelton, A. H. White, P. A. White, *Aust. J. Chem.* **1997**, 50, 959.
- [47] G. B. Deacon, R. N. M. Smith, *Russ. J. Org. Chem.* **1982**, 1584.
- [48] C. C. Hunt, J. R. Doyle, *Inorg. Nucl. Chem. Lett.* **1966**, 2, 283.
- [49] R. H. Crabtree, A. Gautier, G. Giordano, T. Khan, *J. Organomet. Chem.* **1977**, 141, 113.
- [50] R. H. Blessing, *J. Appl. Crystallogr.* **1997**, 30, 421.
- [51] G. M. Sheldrick, *SHELX 97, Program for Crystal Structure Determination*, Universität Göttingen, **1997**.

Received: October 27, 2000 [F2829]